EFFECT TYPE OF CONDUCTIVE INK TO STRETCHABLE PRINTED CIRCUIT UNDER THERMAL PERFORMANCE

NURUL SYAFIKA BT ROZALI

A report submitted

in fulfilment of the requirement for the degree of

Bachelor of Mechanical Engineering (with Honours)

Faculty of Mechanical Engineering

UNIVERSITI TEKNIKAL MALAYSIA MELAKA

2018

DECLARATION

I declare that the project entitled “Effect Type of Conductive Ink to Stretchable Printed Circuit under Thermal Performance” is the result of my own work except as cited in the references.

Signature : .....

Name : Nurul Syafika Binti Rozali

Date : .....

APPROVAL

I hereby declare that I have read this project report and in my opinion, this report is sufficient in terms of scope and quality for the award of the degree of Bachelor of Mechanical Engineering.

Signature : .....

Supervisor's Name : .....

Date : .....

DEDICATION

I dedicated this thesis to my beloved family.

ABSTRACT

Polymer-based electrically conductive inks become as essential elements in flexible and stretchable electronics. The electrically stretchable conductive inks have been applied in various fields such as in biomedical, which is to detect the hydration of athlete's body. Stretchable conductive inks were also used in electronic devices and textile application due to the specialities that can withstand high stress conditions and tend towards high temperature. In order to develop stretchable conductive inks that have good electrical properties by considering the cost of production, further investigation must be done on the properties of the conductive ink. This study seeks to investigate the effects of thermal and mechanical test on sheet resistance of the conductive inks. This study also presents on how weight percentage of filler loading affected the resistivity. This study is focusing on the measurement of sheet resistance for two different types of conductive inks, which are carbon black and singlewalled carbon nanotubes by using four-point probe system and referred ASTM F390 as a guideline. Thermoplastic polyurethane was used as the substrate. For the thermal test, the samples were exposed to the four different level of temperature - 32 °C (room temperature), 40 °C, 60 °C and 100 °C. Hair dryer was used as tool to supply heat since it is easy to handle and can control the level of heat easily. Next, for the mechanical test, it is includes of strain test at 20 %, 40 %, 60 % and 80 % of elongation in room temperature condition. The strain test is conducted by using vernier callipers as a tool to provide strain. Scanning Electron Microscope (SEM) was used to analyzed the surface morphology and the determination wt.% of filler loading for both inks. As a result, it was found that sheet resistance of conductive ink were decreased as the temperature applied increase. However, for the strain test, sheet resistance increase with the increasing of strain applied. Eventually, the higher wt.% of filler loading contained in the conductive ink, the lower the sheet resistance value.

ABSTRAK

Dakwat konduktif yang berasaskan polimer menjadi elemen penting dalam elekronik yang bersifat kebolehlenturan dan boleh diregang. Dakwat konduktif boleh diregang telah digunakan dalam pelbagai bidang seperti dalam bidang bioperubatan, iaitu untuk mengesan penghidratan yang berlaku pada badan atlet. Seterusnya, ia juga digunakan dalam peranti elektronik dan aplikasi tekstil oleh kerana keistimewaannya yang dapat menahan keadaan yang bertekanan tinggi dan cenderung ke arah suhu yang tinggi. Untuk menghasilkan dakwat konduktif yang boleh diregang dan mempunyai sifat elektrik yang baik dengan mengambil kira kos pengeluaran, kajian yang lebih lanjut harus dilakukan ke atas sifat-sifat dakwat konduktif. Kajian ini adalah bertujuan untuk menkaji kesan ujian haba dan mekanikal ke atas rintangan elektrik dakwat konduktif. Selain itu, kajian ini juga membincangkan tentang bagaimana peratusan berat pemuatan pengisi mempengaruhi rintangan. Fokus kajian ini adalah terhadap pengukuran bacaan rintangan bagi dua jenis dakwat konduktif yang berbeza, iaitu karbon hitam dan karbon nanotiub berdinding tunggal dengan menggunakan sistem probe empat titik, dengan merujuk kepada ASTM F390 sebagai garis panduan. Termoplastik Poliuretana digunakan sebagai substrat. Bagi kajian haba, sampel didedahkan kepada empat suhu yang berbeza – 32 ° C (suhu bilik), 40 ° C, 60 ° C dan 100 ° C. Pengering rambut digunakan sebagai alat untuk membekalkan haba kerana ia mudah dikendalikan dan dapat mengawal tahap haba yang dibekalkan dengan mudah. Seterusnya, bagi ujian mekanikal, ia termasuk ujian ketegangan pada 20 %, 40 %, 60 % dan 80 % pemanjangan dalam keadaan suhu bilik. Ujian ketegangan dilakukan dengan menggunakan angkup vernier sebagai alat untuk memberikan regangan. Mikroskop pengimbas elektron (SEM) digunakan untuk menganalisis permukaan morfologi dan menentukan wt.% pemuatan pengisi untuk kedua-dua dakwat. Hasil menunjukkan rintangan dakwat konduktif telah menurun apabila suhu yang dikenakan ke atas sampel meningkat. Walau bagaimanapun, bagi ujian ketegangan, didapati bahawa rintangan meningkat dengan peningkatan tahap rengangan yang dikenakan ke atas dakwat konduktif. Akhir sekali, semakin tinggi nilai peratusan berat pemuatan pengisi di dalam dakwat konduktif, semakin rendah nilai rintangan dihasilkan.

ACKNOWLEDGEMENTS

Firstly, I would like thank to Allah Almighty for gave me strength and blessing that allowed me to complete this research within the time given. Next, I would like to take this chance to express the deepest appreciation to my supervisor, Dr. Mohd Zaid Bin Akop, who was continuously give advice, support and spending his valuable time and energy to make this research complete successfully. It is a great honour to work under his supervision. I am very thankful for having such a good adviser like you.

I would like to express my sincere gratitude to my family members for their encouragement and always support me in doing this research. Very special thanks to my group members, Nurul Hasanah Binti Sobri, Muhammad Aiman Bin Suhaimi, Muhammad Zaim Bin Azmi, Abdul Mueezz Bin Abdul Raheem and Muhammad Amin Bin Othman for their invaluable help and kind endless help.

Lastly, I humbly extend my thanks to Siti Ashikin Binti Azli, master degree student who always give guidance and sharing knowledge especially to conduct the experiment.

TABLE OF CONTENTS

LIST OF TABLES

LIST OF FIGURES

LIST OF APPENDICES

LIST OF ABBREVATIONS

SPC	Stretchable Printed Circuit
PCB	Printed Circuit Board
SWCNTs	Singlewalled Carbon Nanotubes
MWCNTs	Multiwalled Carbon Nanotubes
CB	Carbon Black
TPUs	Thermoplastic Polyurethanes
PDMS	Polydimethylsiloxane
RT	Room Temperature
SEM	Scanning Electron Microscopy
CNTs	Carbon Nanotubes
TPEs	Thermoplastic Elastomers
SS	Soft Segments
HD	Hard Segments
T	Temperature
RT	Room Temperature

LIST OF SYMBOLS

wt.%	-	Weight percentage
Ag	-	Silver
Mg	-	Magnesium
Si	-	Silica
Rs	-	Sheet resistance
I	-	Current
V	-	Voltage

CHAPTER 1

INTRODUCTION

1.1 Background

The 1950s was a decade of the stretchable circuit was introduced in a very limited and slight way. It is also can be known as stretchable printed circuit (SPC). The simplest definition for stretchable printed circuit is a pattern of conductive traces bonded on stretchable substrates and in other words, it is a perfect solution for electronics packaging needs. Due to its capabilities and reliability, stretchable printed circuit has a valuable position compared to traditional printed circuit in worldwide printed circuits market. Stretchable printed circuit are being used widely in everyday technology and electronics in addition to high-end, complex completed components. The usage of SPC in modern portable electronics, hard disk and desktop printers are a few of the most outstanding examples.

Nowadays, stretchable printed circuit is mainly used in small or thin electronic institution compared to traditional printed circuit board. It is due to several good features of stretchable printed circuit compared to traditional printed circuit board (PCB). The first one is, SPC is highly stretchable and foldable compared to traditional PCB that is rigid. Next, stretchable printed circuit can be folding without affecting the signal transfer function. Application of the product also will be reduce, significantly reduce weight, increase function, cost reduction. Besides, printed circuit also anti-vibration due to the

added flexibility and lighter weights allow the printed circuit to absorb and reduce the impact of the vibration to itself as well as any solder joints in connections. Stretchable printed circuit also can be use in harsh environment because it is built with materials that are have the waterproof, moisture proof, shock proof, high temperature oil and corrosion resistance properties.

In general, stretchable printed circuit comprising of filler, binder, solvent and substrate. There are a lot of different type of conductive filler that has being use in industry for example singlewalled carbon nanotubes (SWCNTs), multiwalled carbon nanotubes (MWCNTs), carbon black (CB), silver and graphene. Solvent also one of the important substances in the stretchable printed circuit that will increase the cross-linking of polymer. Cross-link is bond that links one polymer chain to another. Next, it is also a variety of material for improved thermal physical and chemical properties. Binder is a polymer, which for particle redistribution and restoration of conductivity upon solvent evaporation for example epoxy and resin. There are a few types of flexible substrate that has been used for example Thermoplastic Polyurethanes (TPUs) and Polydimethylsiloxane (PDMS).

Conductive inks are a mixture of conductive particles or filler, polymer binders, and dispersing solvents. The combination of the three elements will form conductive ink, which conducts electricity. They have been used in many electronics in industry for example in metallization of microcircuits, solar cells, large area electronic structures, and solder for microelectronics packages. Other than that, it is also technologies that compatible with many substrate surfaces including polyester, glass, and ceramics, and can be applied using screen.

This research will focus on the different types of conductive inks in stretchable printed circuit. Different conductive inks will have different properties. In other words, they will have the different in mechanical, thermal and physical properties that will affect the electrical conductivity of the conductive ink. The goal of this study is to investigate the effect thermal and strain on sheet resistance of different type's conductive ink.

In electronic industry, good conductivity of polymer-based conductive ink plays a big role that related to cost effective. Thermal conductivity that can be defines as a property of a material's ability to conduct heat while thermal resistance is a measure of a material's ability to prevent heat from flowing through it. In the other words, the greater conductivity, the lower its resistance.

1.2 Problem Statement

Over the past few years, in order to improve and upgrade the industry technologies, printed circuit board is invented from rigid printed circuit board to stretchable printed circuit board. This is due to the limitation of the usage rigid printed circuit in industry for example it has fixed mode or shape depending on the shape of the product, rigid and has no anti-vibration. The fixed board is replaced by flexible substrate since it has flexible and stretchable properties. Conductive inks that are both stretchable and flexible are performing as better application in stretchable printed circuit electronic devices. Therefore, the demand of highly flexible and bendable of printed circuit is grow rapidly. To have high quality of stretchable conductive ink, it must be able to expose with high level of temperature, capable on has good adhesive strength with the substrate while maintaining the electrical conductive performance. However, the current stretchable conductive ink have their own weakness which is it only can bend along single axis and cannot be comply

with arbitrary shapes like for example surface texture of human skin. It is significant to do the further study on the effect of mechanical test to the electrical performance of the conductive ink while making it is suitable to be applied in high performance application. In this study, the mechanical test includes of strain for several elongation.

Next, the electrical performances, which are the conductivity of the stretchable conductive ink, also have certain limitation under the thermal application. As mention before, in order to improve the standard of the stretchable conductive ink, it must be able to be implemented at high temperature conditions. Therefore, it is very important to investigate the particle's behavior of the conductive ink and compatibility between inks with the substrate since the physical properties of the substrate might affect the performance of the stretchable conductive ink. The conductive ink that has been used in this study are singlewalled carbon nanotubes and carbon black, which has their own properties.

These problems will be study based on several parameters for example the effect of temperature and strain towards the resistivity of the conductive inks. Therefore, this research will cover on the effect of different type of conductive ink to stretchable printed circuit under thermal performance. CB and SWCNTs has been used to improve and enhance a better quality of stretchable printed circuit. Next, the aim of this study is to conduct experiment by using SWCNTs and CB that have a better conductivity and high strength in different condition applied.

1.3 Research Objective

The objectives for pursuing the current research topic are:

1. To determine the effect of temperature to sheet resistance of CB and SWCNTs for enhance the material properties.
2. To study the effects of strains to the sheet resistance of CB and SWCNTs at room temperature for upgrade the functionality.
3. To study the effects weight percentage of filler loading in the conductive inks to the sheet resistance for improve the electrical performances.

1.4 Scope of Project

The scopes of this project are listed as below:

1. Screen printing of conductive ink on TPUs substrate.
2. Measure sheet resistance of conductive ink using four-point probe:
    - Elevated temperature at 32 °C (RT), 40 °C, 60 °C and 100 °C
    - Strain at 20 %, 40 %, 60 % and 80 % of elongation
3. Surface morphology study by using SEM analysis.

1.5 Planning and Execution

The details of research activities for PSM I are shown as in Figure 1.1 below. Figure below illustrates the research activities for PSM 1 that includes the process of research title selection, literature review, designing the experiment, pre-experiment, formulation of samples, material characterization testing for thermal analysis, data validation, report writing and followed by report submission and lastly PSM I Seminar. The material characterization includes mechanical and thermal testing.

Week / Activities	1	2	3	4	5	6	7	8	9	10	11	12	13	14
Research Title Selection														
Literature Review														
Design of Experiment														
Pre-experiment														
Formulation of Sample														
Characterization Testing i. Thermal														
Data Validation														
PSM I Report Writing														
PSM I Report Submission														
PSM I Seminar														

Figure 1.1: Gantt Chart for PSM I Activities

For PSM II, the research activities started with the sample preparation for both conductive inks, which are CB and SWCNTs. Next, the activity is followed by the surface morphology study by using Scanning Electron Microscopy (SEM) analysis, characterization testing under thermal and mechanical test. SEM analysis was study to analyze the particles content in the both conductive inks. The thermal test includes of supplying elevated temperature to the samples starting with 40 °C, 60 °C and 100 °C. For the mechanical test, it is includes of applying strain at 20%, 40%, 60% and 80% of elongation to the samples. After all the testing completed, proceed with the data analysis, result and discussion. The research activities for PSM II stage are detailed out as in Figure 1.2 below.

Week / Activities	1	2	3	4	5	6	7	8	9	10	11	12	13	14	15
Sample Preparation i. Carbon black ii. SWCNTs															
Morphology Study															
Characterization Testing i. Thermal ii. Mechanical															
Data Analysis															
Result and Discussion															
PSM II Report Writing															
PSM II Report Submission															
PSM II Seminar															

Figure 1.2: Gantt Chart of Activity Details and Their Respected Time Frame for PSM II

CHAPTER 2

LITERATURE REVIEW

2.1 Introduction

In this chapter, a review on conductive ink, filler, substrate, four-point probe system and the properties of the conductive ink including thermal, electrical and physical properties have been discussed further.

2.2 Conductive Ink

Conductive ink plays a big role in stretchable printed circuit. The definition of conductive in electrical view is the ability of the material or substances to conduct electricity. With high conductivity of the material, such as metal, the electric current will able to flow easily when voltage is exerted. It is also simply stated by D. Banfield (2000), material with lower resistance will conduct electricity more efficiently compared to material that has high resistance. Electrical resistivity or in other words, specific electrical resistance is a parameter to measure how potentially conductors to resist the flow of electric current. Next, the conductivity is inversely proportional to the resistivity, which is high conductivity of conductor or material will results a lower resistivity.

Nowadays, the market and manufacture conductive ink showing sign of growth due the high demand in industries. It is use in various type of industries such as industries of

manufacturing switches, flexible printed circuit board, telephone equipment, printed switches and heating elements (Cargill et al., 2004). Conductive ink is an ink that printed on object or substrate, which gives a functional of conduction that the ability of the electrical charge carriers (electrons), move efficiently from atom to atom and simply defined as conducts electricity. Besides, it is a conductive element used in electronic applications to provide stable electrical interconnections. For the flexible printed circuit, the conductive inks layer is built up or has been printed on a polymer substrate. Polymer-substrate is one of the polymer-based electrically conductive inks and that has been used widely in electrical industries (Banfield, 2000). It is used to make the conductive paths on the substrate. There are several types of substrate that able to be used as polymer-based electrically such as Thermoplastic Polyurethanes (TPUs) and Polydimethylsiloxane (PDMS).

In essence, conductive ink comprises three substances, which are filler, binder and solvent (Odom et al., 2012):

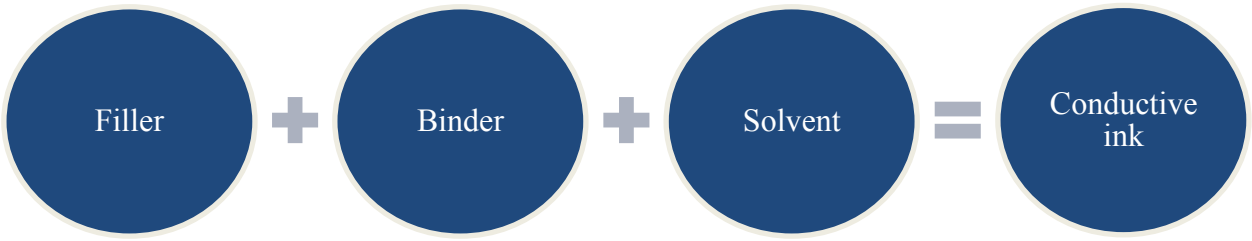

Figure 2.1: Components in Conductive Ink

The common filler that has been used is silver (Ag) conductive filler (Merilampi, Laine-Ma, & Ruuskanen, 2009). There are another conductive filler widely used in electronic devices include of carbon black and nanoparticles. Singlewalled carbon nanotubes (SWCNTs) and multiwalled carbon nanotubes (MWCNTs) are known as nanoparticles. Next, usually thermoplastics and epoxy are use as the binder in the conductive inks. According to the various research (Banfield, 2000 ; Jacobson et al., 2015), the functions of the binder in the conductive inks are to hold the conductive filler particles together that is to ensure the conductive filler stick to the polymer-substrate and provide the final dried film strength and adhesion to a given substrate. The binder applied is depends on the polymer-substrate and solvent that has been used. Next, conductive inks also contained of solvents. The binder will be dissolved in the solvents and the others role of the solvent in the conductive ink are to be a controller of the drying rate and to convert the binder into a liquid. The filler is able to be mixed in and can be screen printed if it is in a liquid form (Banfield, 2000).

There are several parameters that can affected the performance of sheet resistance, Rs (Ω/sq) of the film which includes of force applied (tension) and temperature applied to the film. Temperature applied will influence the particle radius of the conductive filler more precise and will affect the electrical conductivity of the conductive ink. In addition, the percentage of tension applied to the conductive ink also will affected the sheet resistance since there will be changes on the gap between particles in the conductive filler. In these cases, sheet resistance is measured by using four-point probe system.

2.3 Filler

In the developing countries, it is important to produce product with higher efficiency, high sustainably and affordable. Thus, important features need to be considered in order to enhance the properties of the product. For this study, it is related to the stretchable printed circuit. There are several important features must be review in order to improve the quality of the circuit. The features includes of low manufacturing costs, high durability and high efficiency. In order to meet the requirements of the features, it is necessary to choose high quality of the materials. High quality of material is strongly related to the several properties for example mechanical and electrical properties. Mechanical properties includes of elasticity and tensile strength while electrical properties can be known as sheet resistance and thermal conductivity.

Conductive filler is one of the main components in the stretchable printed circuit. Conductive filler provide electrical conductivity to the circuits and form a conductive ink when it is combining with the binder and solvent (Merilampi et al., 2009). Commonly, silver particles are used as the conductive filler material. However, in this study, carbon black and nanoparticles, which is singlewalled carbon nanotubes (SWCNTs), have been used as the conductive filler due to their good properties. According to Thostenson (2001), nanoparticles such as carbon nanotubes have unique electronics properties and high conductivity compared to diamond also the mechanical properties of the material such as stiffness and strength is better than any currents materials. This is one of the factors for choosing nanotubes (singlewalled carbon nanotubes) as conductive filler in this study and will be discuss further to understand their good properties. Table 2.1 below shows the value of thermal conductivity of various conductive filler (Han & Fina, 2011). From the Table 2.1, it shows that carbon nanotubes have the highest value of thermal conductivity where carbon black has the lowest value of conductivity.

Table 2.1: Thermal Conductivity of Conductive Filler

Material	Thermal Conductivity at 25°C (W/mK)
Carbon Nanotubes	2000~6000
Diamond	2000
Copper	483
Silver	450
Gold	345
Carbon black	6~174

2.3.1 Carbon Black

Carbon black is well known as the traditional carbon based fillers and has been widely use. As stated in many of research, carbon based filler be present as the conductive filler which has high thermal conductivity (good in electrical properties) and light in weight (Han & Fina, 2011). Carbon black is not only good in electrical properties, which is has low in resistivity, they are also popular in electronic manufactures since carbon black also low in cost and high chemical stability (Pu et al., 2014). Their electrical conductivity has been improved day by day.

Current analysis produced carbon black with high conductivity and having a very high surface area (Nanda, 2008). Thus, it is lead to the better electrical conductivity. Carbon black is form in aggregates of graphite. It also mentioned by Technology (2013), carbon black is composed of small functional unit which called as aggregates. The particles are ‘aggregates’ to each other by Van der Waals forces. The forces hold sheets together and provide less or more unbreakable bond. The graphite that exist in carbon are as microcrystal particles and the characteristic of their particles size are around 10 – 500 nm.

Next, the surface area of the particles are around 25 – 150 m^2/g (Han & Fina, 2011). Carbon black also composed of hexagonal and pentagonal faces. According to Han & Fina (2011), it is stated that carbon black provide better electrical conductivity instead of thermal conductivity.

In addition, carbon black experiences of high structure and very high surface area as mention before. Therefore, the complex structure of the branch filler aggregates provide a strong surface polymer interaction leading to higher bound. The cross-linking will increase next will increase in hardness.

As the carbon nanotubes, the higher the temperature apply to the carbon, the lower the sheet resistivity value since the gap between particles in the conductive ink will decrease (Hasnaoui et al., 2017). When heat is applied, it will cause the particles of conductive filler expand and will reduce the gap between the fillers. Next, the electron will flow easily since the conductive fillers have more contact area between each other and will increase the conductivity of the conductive ink (Banfield, 2000). This statement can be simple illustrated as Figure 2.2 below:

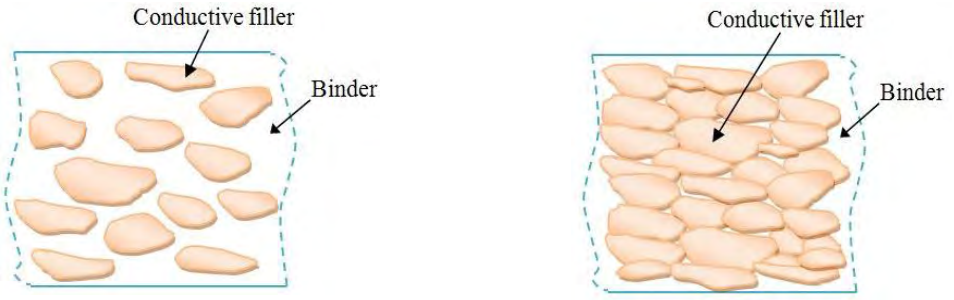

(a) Before heat (b) After heated

Figure 2.2: Illustration of Conductive Particle Filler after Heat Applied

For the strain, they will have inversely result as the temperature applied. Commonly, if the ink does not have good adhesion properties, they will tear apart after 100% of strain applied. Since the ink has been tearing up, the electron will fail to flow. In a simplest sentence, the sheet resistance will increase. Generally, carbon black has low thermal conductivity compared to other conductive filler. Since carbon is low in cost, hence this is one of the reasons for choosing this material as conductive filler in this study.

2.3.2 Nanoparticles

Nanoparticles are at the leading edge of the rapidly developing field of nanotechnology. The addition of nanofillers with highest thermal conductivity becomes the newest interest to enhance the thermal conductivity of polymers. Due to the advance properties of the nanoparticles, carbon nanotubes (CNTs) that has outstanding thermal conductivity, CNTs is the finest material guarantee for thermal conductive composites (Thostenson, 2001). Thus, CNTs is one of the crucial elements in the stretchable printed circuit since they will provide electrical conductivity. To maintain the good potential of SPC, fully understanding about the CNTs includes of their elasticity, fracture properties, thermal conductivity and resistivity must be performed. Many researchers have confirmed that mechanical, thermal and electrical properties of CNTs outperform those any in the past materials. Next, an electric current carrying capacity 1000 times higher than copper. CNTs also exhibits low sheet resistance (Ho & Wei, 2013).

Carbon nanotubes can be visualized where sheets of graphite are built up by rolled into a tube. Graphite is the most stable form of crystalline in carbon. The atomic structure of CNTs also can be expressed with respect to the tube chirality or helicity. Chirality of the structure also can defined the properties of the CNTs either metallic or semiconductor.

Thermal conductivity of CNTs also can be affected by the atomic structure or arrangement, tube size, and morphology of the nanotubes (Vaccarini et al., 2000). According to Che et al., (2000), it is stated that conductivity on CNTs also depends on how the sheets of graphite are rolled, length and diameter of the tubes. CNTs atomic structure can be illustrated as Figure 2.3 below:

(a) Armchair Nanotubes (b) Zig-zag Nanotubes

Figure 2.3: Illustration of CNTs Atomic Structure (Han & Fina, 2011)

Next, CNTs have been widely used in many applications since it is categorized as extraordinary electronics and the thermal conductive exceeds thermal conductivity of diamond that is twice as high as diamond. In accordance with (Han & Fina, 2011), at room temperature, for a single nanotubes, carbon nanotubes can be experienced longitudinal thermal conductivity of 2000 – 6000 W/mK and might be increase with increasing temperature. Experimental results from (Thostenson, 2001), it shows that CNTs has notably high value in elastic modulus, which is greater than 1 TPa whereas diamond has elastic modulus of 1.2 TPa. Besides, it is also recorded that the strengths of CNTs is 10 - 100 times higher than the strongest steel. They also have simulations, which prove that the CNTs are outstandingly can experience extreme strain without signs of brittleness. This

statement is strongly supported by (Vaccarini et al., 2000), it is stated that CNTs has excellent stiffness and bending flexibility. These properties strengthen the reveal of the ability of CNTs to sustain high percent of strains without fail. CNTs also can withstand superior thermal properties, which is thermally stable up to 2800 °C in vacuum.

As mention before, several properties of carbon nanotubes such as electrical and mechanical properties are depending on the atomic arrangement of the structure. Other than that, different atomic arrangement also can form various types of CNTs for example singlewalled carbon nanotubes and multiwalled carbon nanotubes. MWCNTs are simply made of concentric single-walled carbon nanotubes. Nanotubes come out as extraordinarily graphitized, which is sp basic structural unit carbon bonded chains. Both nanocarbons are form of arrangement of carbon atom on each shell with variety degrees of chirality and chapped with pentagons. Figure 2.4 below shows the structure of SWCNTs and MWCNTs.

(a) SWCNTs (b) MWCNTs

Figure 2.4: Atomic Arrangement of Singlewalled and Multiwalled CNTs ("All Leaflet.Pdf," n.d.)

For this study, it will be focusing on the effect of thermal and percentage of strain applied on the conductivity of stretchable printed circuit. According to Oskouyi et al., (2014), the resistance of the composite is inversely proportional to the temperature. It also

can be expressed as the higher the temperature applied, the lower the Rs value, means that the higher the conductivity of the sample as the resistivity is inverse of conductivity. This is due to the increase of the charger carrier in the structure (Hasnaoui et al., 2017).

2.3.2.1 Singlewalled Carbon Nanotubes

Singlewalled carbon nanotubes are widely known because it have been proved that possesses significant and high engineering interest because of their speciality in electrical and thermal properties. SWCNTs is one of the nanotubes which are rolled up from graphite sheet into cylinders to form closed cylinders with hemispherical cap. Singlewalled carbon nanotubes composed of tubes with an armchair atomic structure. Next, is also containing carbon which are in sp^2 bonded carbon, forming hexagonal lattice with diameter of length between 1 - 2 nm (Kiang et al., 1995). Sp^2 bonded carbon gives insulating behaviour and special electronic structure to the conductive ink. Theoretical research of nanotubes have been revised, which they will experience extraordinary mechanical, electrical and thermal properties of basic scientific importance and possible to be one of the technology importance. The mechanical properties of SWCNTs is expected to be exceed those of any current material (Thostenson, 2001).

SWCNTs can withstand high angle of bending. Simulation shows the bending angle is up to 110°. The simulation proved that SWCNTs could experience big angle of bending as shown in Figure 2.5. From the simulation, it shows that SWCNTs can undergo exceptionally large breaking strain, which is percent of strain about 30 - 40 % (Thostenson, 2001; Ho & Wei, 2013). Next, the breaking strain decrease as the temperature decrease. Vaccarini et al. (2000) stated that carbon nanotubes is one of the material that has a lightweight and very high value of Young's Modulus since they are arranged in ropes and

closely pack stacking. The value of the Young's is approximately 1 TPa almost same as diamond. The density of the SWCNTs is depends on the chirality or helicity of the atomic structure. The density value is in range from 1.33 g/cm^3 to 1.40 g/cm^3 (Mantena et al., 2008). Next, the chirality also can defined either the nanotubes is metallic or semiconductor.

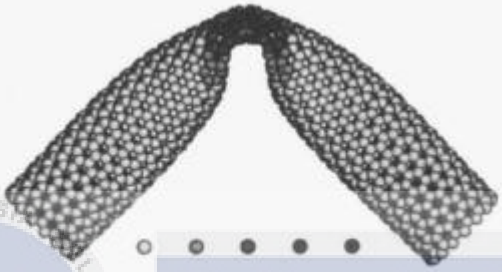

Figure 2.5: Simulation of SWCNTs Buckling (Thostenson, 2001)

The thermal conductivity can be affected by temperature. Lukes & Zhong (2007) stated that, the higher the temperature, the higher the thermal conductivity of the ink. Thus, the higher the temperature applied, the lower the value of sheet resistance until it is achieved their maximum limit of temperature. Commonly, the thermal conductivity of singlewalled carbon nanotubes is around 2000 - 6000 W/mK at room temperature (Han & Fina, 2011). Since the thermal conductivity is depends on the diameter of the tubes, atomic arrangement of the structure and the morphology, hence it is prove that temperature also will affect the conductivity of the CNTs. This is due to the diameter of the tubes, atomic arrangement of the structure and the morphology of SWCNTs might change when temperature is applied.

2.3.3 Weight Percentage of Filler Loading

The electrical resistivity of conductive ink may be affected by the weight percentage (wt.%) of fillers either for carbon black or for singlewalled carbon nanotubes. In recent years, the electrical performance of the polymers filled with carbon nanotubes have been extensively studied by many researchers. According to Chung et al., (1982), the resistivity of the conductive ink decrease as the higher wt.% of fillers contained in the ink. In placing more emphasis, Lin & Chung (2007) claimed that the degree of conductance of the conductive ink increase with the increasing of fillers content. Thus, increasing fillers particles in the conductive ink leads to increasing numbers of electrical interconnections and the clusters of the fillers contribute to the transition of the ink from insulator to conductor. This phenomenon can be known as percolation threshold where the transition occurs and provide percolation network to let the current pass through across the ink (Oskouyi et al., 2014).

The particles of filler must be appropriately dispersed over the matrix, means that the conductive material initiate particle to particle to contact each other and allow the electrical conductivity phenomena occurred. As a result, by contacting to each particle, it will provide space for electrons to move throughout and will improve the electrical conductivity. In order to have better network of the filler particles, it is necessary to consider another parameters for examples size of the particles, particle geometry and the distribution ways (Trinidad, 2016) . Due to excessive filler contents and small amount of polymer in the conductive ink, it might produce poor adhesion properties in the ink. Thus, due to the poor adhesion properties, it will cause the surface of the conductive ink crack after certain limit of heat is applied (Dziedzic et al., 1993).

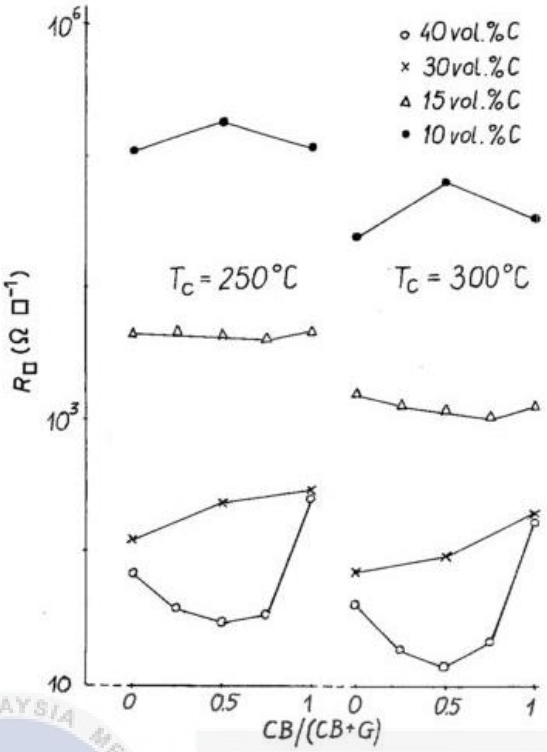

Figure 2.6: Sheet Resistance Versus Contents of Active Phase for Several Volume Fraction of CB Fillers at Different Curing Temperature (Dziedzic et al., 1993)

From Figure 2.6 above, it shows the relationship between amount of carbon black fillers and the sheet resistance. The decrease of Rs is due to the increasing number of fillers in the conductive ink. 40 vol. % of CB in the conductive ink resulted the lowest value of sheet resistance while 10 vol. % of CB gives the highest reading of sheet resistance. It is prove that, the higher volume fraction of filler produce better conductivity of material. This statement can also be supported by similar research done by (Han & Fina, 2011) for the CNTs, the finding has shown that the electrical conductivity of the carbon nanotubes improved by adding more fillers in the inks. As shown in Figure 2.7 below, it is result for thermal conductivity versus CNTs loading. The electrical conductivity of CNTs increase as the weight percentage of filler loading increases. In other word, the higher weight

percentage filler results the higher volume percentage of the filler. Hence, as mentioned before, volume percentage of fillers is directly proportional to the electrical conductivity.

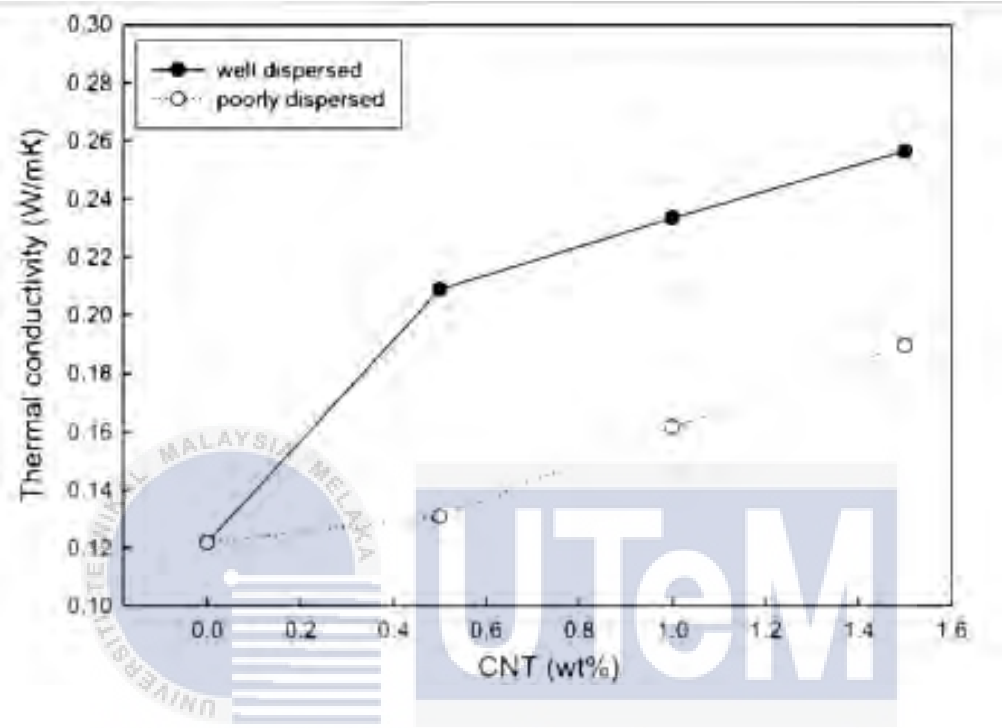

Figure 2.7: Thermal Conductivity Versus Weight Percentage of CNTs for Well and Poorly Dispersed (Han & Fina, 2011)

2.4 Substrate

In these times, most of the electronic industries more prefer to use stretchable printed circuit board instead of rigid printed circuit. This is due to the features of the SPC better than rigid PCB. One of the disadvantages of the rigid PCB is they are not able to be bending and they are not stretchable where SPC can be both stretchable and bendable. In facts, a stretchable electrical device possesses high mechanical stretchability compared to rigid electrical devices (Hocheng & Chen, 2014) . The printed circuit become flexible and stretchable circuit since the non-conductive substrate and copper layers has been replaced with polymer-substrate. The printed circuit can be illustrated as in Figure 2.8.

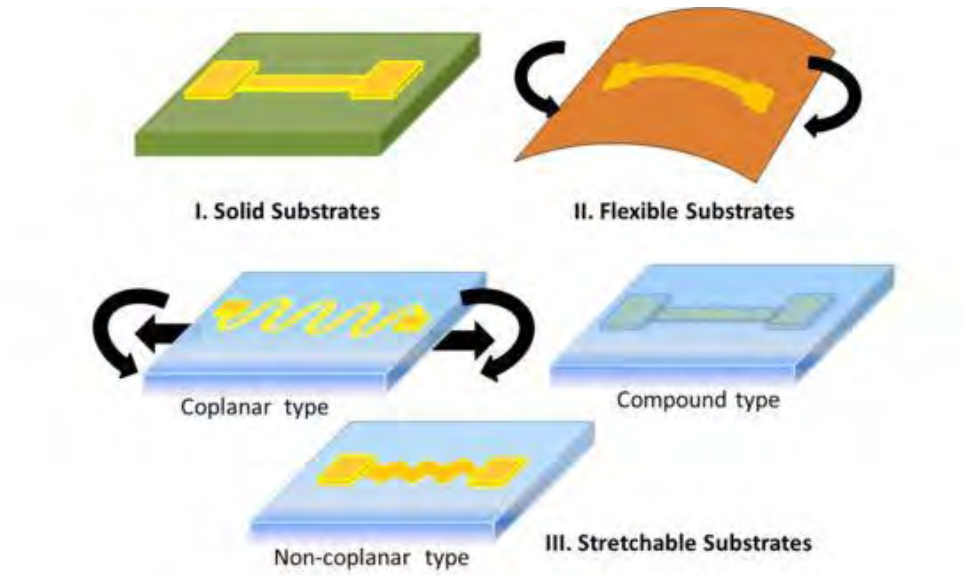

Figure 2.8: Solid Substrates, Flexible Substrates and Stretchable Substrates (Hocheng & Chen, 2014)

Since the rigid PCB using firm and solid substrates due to the high strength against impacts and bending load, hence they are dominating in reliability among of the three printed circuits. Next, for the flexible PCB, they use flexible substrate and has a limitation in bendability and lower in stretchability compared to SPC. Their lifespan also will dramatically decrease as the circuit being folded for a thousand cycles. Even though stretchable printed circuits can experience large bending and stretching action, it could also can be applied in non-planar surface. However, they have a short lifespan among the three due to the working condition for example being bent and stretch frequently (Hocheng & Chen, 2014). The stretchability of the circuits or electronics can be applied in various fields for example biomedical and textile applications. Next, they also can be placed in human skin, which able to be adjust to the curvilinear surface. This technology could determine

and detect the hydration of athlete's body during the training session (Suikkola, 2015). Stretchable and rigid interconnects can be simple illustrated as in Figure 2.9.

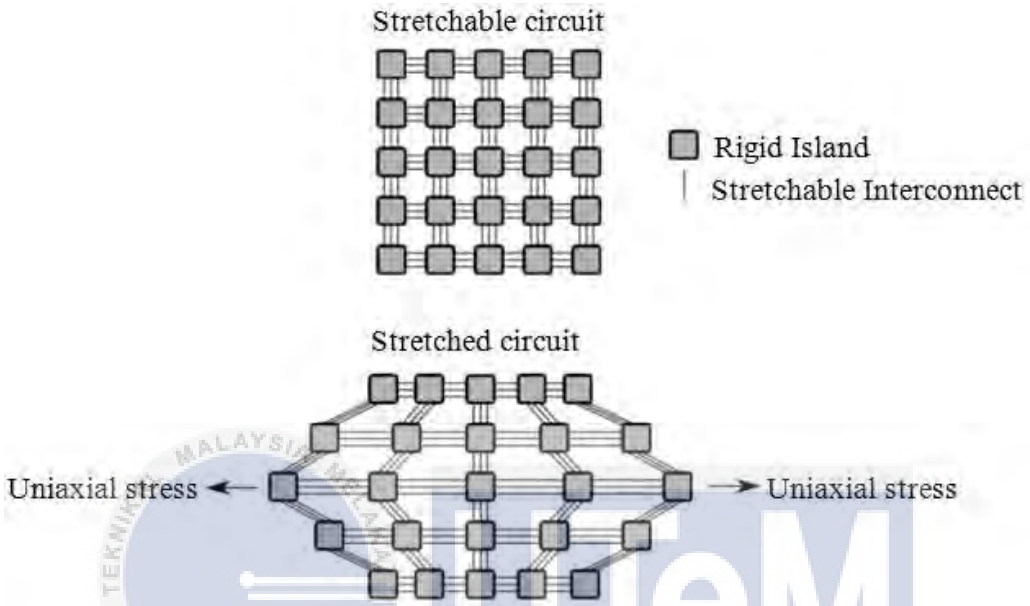

Figure 2.9: A hybrid Circuit Consisting of Rigid Island and Stretchable Interconnect (Suikkola, 2015)

The illustration more precisely defined by the way of the stretchable electronic circuit implemented by initially make in a small sizes (miniaturizing) each of the functional module to a small in size island of rigid PCB. Next, all the islands are linked using glue to the stretchable printed circuit. Thus, the bonds between the islands are complete by using the stretchable interconnects. Together these elements form a stretchable and bendable circuit.

In designing stretchable electronics, mechanical behaviour of the stretchable interconnects might influence the function, bendability and stretchability of the stretchable electronics. For example in medical and textile applications, it is necessary to know the

limitation of the load applied to the devices. Thus, ensures that the physical properties and elasticity of the substrate is well studied. Elasticity can be defined as the way of material reacts when stress force is applied. It is also refers to the capableness of the material to deform in a non-permanent way it is also referring to the ability of the material to return to its original shape and size (original form) after the stress force is removed. In order to produce a better quality of stretchable interconnects, the material used must have high mechanical deformability and possesses high electrical conductivity thermal conductivity. Besides, the performances of substrate also need to be a study in term of capability operating in varies temperature and under stresses load (Agar, 2011). Most commonly used substrate in electronic devices are Thermoplastic Polyurethanes (TPUs) and Polydimethylsiloxane (PDMS) due to their own capability in thermal and mechanical properties (Suikkola, 2015).

2.4.1 Thermoplastic Polyurethanes

Referring to the Qi & Boyce (2004), Thermoplastic Polyurethanes (TPUs) were been commercialized by Bayer-Fabenfabriken in Germany where in the U.S. the commercialization is by B.F Goodrich in year 1950s. Since the materials experience of high performance characteristic, which are high tear strength, solvent resistance, abrasion resistance, high elongation, tensile strength and highly elastic materials, hence, it is widely used across range of markets and application. These characteristics also contribute to the reason of choosing Thermoplastic Polyurethanes in this study instead of another stretchable substrate. Next, TPUs also has high surface energy. In this study, high surface energy is important for the printing process of the conductive ink because it will improve the possibility of good conductive adhesives between stretchable substrate and the

conductive ink (Suikkola, 2015). In addition, good in surface energy also will help the filler easily stick to the substrate.

According to the Alliance for the Polyurethane Industry (API), TPUs can be characterized as “bridging the gap between rubber and plastics”. This is due to TPUs exhibits the mechanical performance typical of rubber but it also can be processed as Thermoplastics. As mention before, Thermoplastic polyurethanes can be classified as unique category of plastic where it is one of the Thermoplastic Elastomers (TPEs) (Rolf Klein, 2011). TPUs is created when a polyaddition reaction take place between one or more diols and diisocyanate. For preparing TPUs, the types of components used are classified in Table 2.2 below. The diisocyanate components acts as soft and hard segments also provide physical properties of TPUs especially the hard segments. Next, the chain extender will give the TPUs its toughness and hardness.

Table 2.2: TPUs Components (Stephens, n.d.)

Components	General structure
Macroglyco	HO-R’-OH
Chain extender structure	HO-R’’-OH
Diisocyanate	OCN-R-NCO

2.4.1.1 Thermoplastic Polyurethanes Properties

The structure of Thermoplastic Polyurethanes composed of diisocyanate and polyol that reacts under the polyaddition process. Low molecular weight of diols acts as chain extender (Sharma, 2016). TPUs structure consists of segmented block copolymers. This structure composed of hard and soft segments that will generate two phases of microstructure. The length scale of both segments separated is about a few tens of nanometres. The ratio between the hard and soft segments might influence the mechanical, thermal, rheological and adhesion properties of the TPUs. The comprising of hard and soft segments ratio is inversely proportional to the phase separation degree and the secondary linkage between polymer chains. More precisely, the higher amount of hard and soft segment ratio, the lower the phase separation degree and the secondary linkage between polymer chains. Commonly, the degree of phase separation that takes place in the Thermoplastic Polyurethanes is resulting from intrinsic incompatibility between both segments.

The hard segments are made of polar materials. The formations of carbonyl to amino hydrogen bonds from the materials have a tendency to cluster into ordered hard domain while the soft segments composed of amorphous domains. Besides, TPUs structure also contains hydrogen bonds that are the combination between urethane-group hydrogen atoms and carbonyl groups. The temperature behaviours and morphology of TPUs substrate is also influenced by the hydrogen bonding (Stephens, n.d.). Next, infirm hydrogen bonding and structure of chain extrudes are in non-linear form is one of the main factors for low mechanical and tensile properties (Sharma, 2016). Alternating structure of Thermoplastic Polyurethanes, which are both hard and soft segments the hydrogen bond can be simply shown as in Figure 2.10 below.

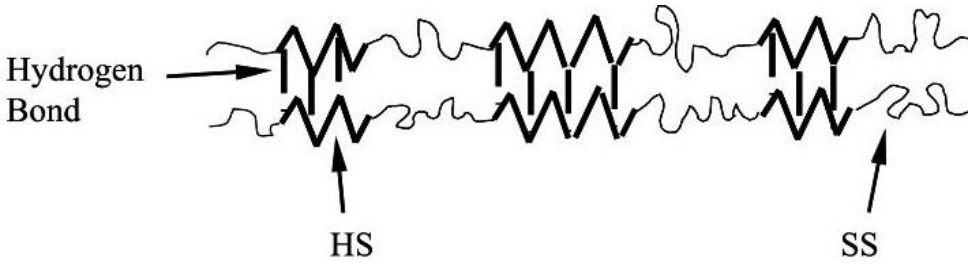

Figure 2.10: TPUs Structure Composes of Soft Segments (SS), Hard Segments (HD) and Hydrogen Bond (Qi & Boyce, 2004)

By referring Figure 2.11 below, it shows the basic chemical components in the Thermoplastic Polyurethanes. The combination of isocyanate chain linked and chain extender forms the hard block, and commonly glassy or semi crystalline in nature, which is function as providing toughness and physical performance properties. However, soft block give different functions to the stretchable substrate and made of different components. The soft block purpose is in term of flexibility, elasticity and elastomeric character of a TPUs substrate that primarily composed of polyols. In nature, it is generally amorphous. In addition, as soft segments molecular weight increase, surface hydrophobicity also will improve (Sharma, 2016). High hydrophobic surface is important because the surface of the substrate will have better contact angle with the conductive ink. The higher the molecular weight of soft segments also will affect the phase of segregation where will be more increase. It will support the TPUs substrate by improve the mechanical properties.

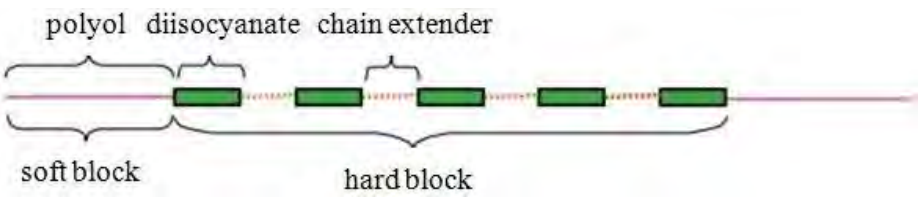

Figure 2.11: Basic Chemistry of TPUs ("A guide to thermoplastic polyurethanes (TPUs)," n.d.)

TPUs are exceptionally has high elasticity; they can withstand strains up to 1000 % but normally, the maximum stress is up to 200 %. The hardness of the Thermoplastic Polyurethanes may be different depends on the types of the polyurethanes. The Ultimate Tensile Strength (UTS) number can value the elasticity of the TPUs, which is 60 MPa. Next, the typical highest temperature limit of the TPUs is at around 120 °C and they possess varies of hardness, from 65 Shore A to 50 Shore D as shown in figure below. For flexible grades, shore A scale recommended is below 92A and the shore D is for rigid grades where the value is above 92A (*A guide to thermoplastic polyurethanes (TPU)*, n.d.).

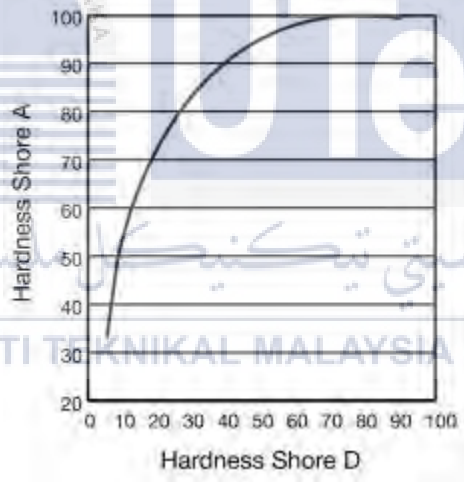

Figure 2.12: The Relationships Shore A to Shore B ("A guide to thermoplastic polyurethanes (TPUs)," n.d.)

It is important to test the characteristics for structural, thermal, surface, and mechanical properties. Mechanical properties can be obtained by applying strain. Next, the thermal properties can be known by apply varies temperature to the substrate. Mechanical and thermal properties is very important in this studies since it is related to the

stretchable printed circuit which is widely used in electronic devices. It is necessary to consider all the properties because the circuits might be use in different environments including harsh environment.

2.5 Four-Point Probe System

Four-point probe has been used in order to measure the sheet resistance in units of ohms per square of conductive ink, Rs. Four-point probe can be used to measure any semiconductor materials both on thin or bulk film specimen. The technique of the four-point probe is where the fixed current is injected into the surface of the conductive ink with constant probes spacing, s (Bautista, 2004). The electrical fixed current, I is supply through the two outer probes while the voltage, V is measured between the two centre probes as shown in Figure 2.13 below. Figure 2.14 shows an image for four-point probe systems from Jandel Company.

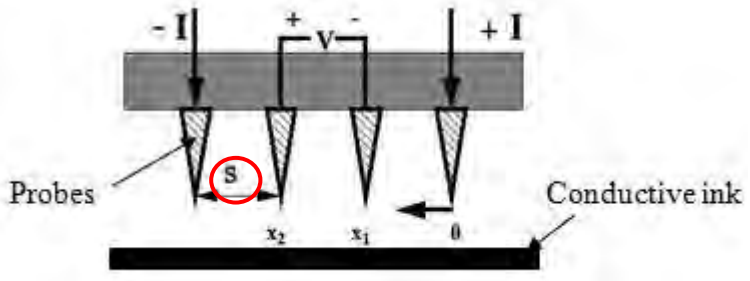

Figure 2.13: Schematic Diagram of Four-Point Probe Configuration (Chan & Friedberg, 2002)

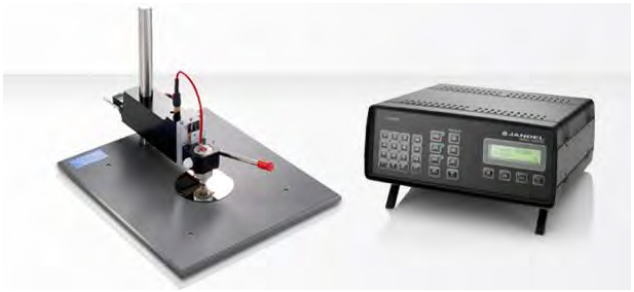

Figure 2.14: Four-Point Probe Systems (Jandel Engineering Four Point Probing System, 2017)

CHAPTER 3

RESEARCH METHODOLOGY

3.1 Overview of Research

In this chapter, the technique of the sample preparation for both conductive ink; carbon black and singlewalled carbon nanotubes, surface morphology analysis by SEM analysis, thermal and mechanical testing and sheet resistance measurement that were conducted during this research project are described. The summary of the methodology for this research is described as in Figure 3.1. The outline of the study is initiated from the literature review of the selected research title until the final thesis writing. The actions that need to be carried out to achieve the objectives in this project are listed as below:

i. Literature review

Journals, articles, or any materials regarding the project will be reviewed.

ii. Design of experiment

This experiment is conducted by using two different conductive ink, which are singlewalled carbon nanotubes (SWCNTs), and carbon black (CB) with Thermoplastic Polyurethanes (TPUs) as substrate. Both inks are ready made.

iii. Curing

For CB, the conductive.ink should be allowed to dry at room temperature for 5 - 15 minutes. Drying time can be reduced by placing the conductive ink under warm lamp or other low intensity heat source. For the SWCNTs, it is cured in oven at controlled temperature. The temperature was set up at 100 °C for 1 minutes.

iv. SEM analysis

Surface morphology study is conducted by using SEM in order to analyse the particle behaviour of the both conductive inks.

v. Measuring resistivity

The sheet resistance, Rs of two different conductive inks was measured by using Four-Point Probe system by referring ASTM F390 (Appendix A). Rs is measure at two different cases, which are the value of Rs at four different temperatures applied - 32 °C, 40 °C, 60 °C and 100 °C. Next, Rs value when strain was applied at 20 %, 40 %, 60 % and 80 % of elongation.

vi. Analysis variable and parameter

Analysis variable and parameter will be presented by analyze the data and compare with theoretical data.

vii. Report writing

A report on this study is written at the end of the project.

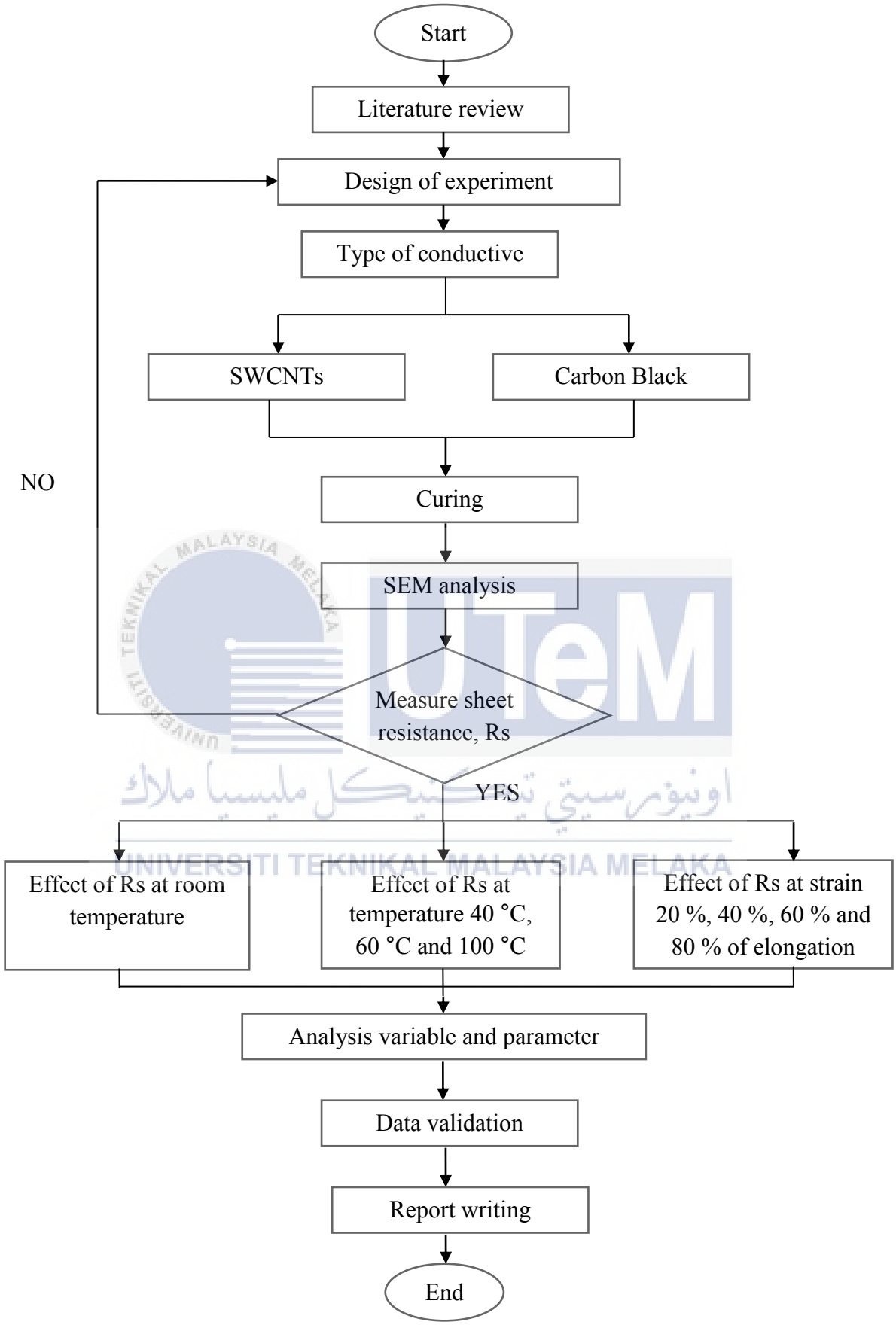

Figure 3.1: Flow Chart of the Methodology

3.2 Materials

3.2.1 Carbon Black (CB)

The readymade carbon black conductive ink was used for this experiment or can be known as Bare Conductive Electric Paint as shown in Figure 3.2. The ink adheres well to wood, paper products, corks, textiles and metal. However, for hydrophobic material such as plastic and glass, CB will exhibit poor adhesion. Next, they are also easily removed by water. The flexibility is depends on two factors. The first one is the layer thickness of the printed conductive ink. A consistently thin layer printed provides circuit that is more flexible. Increasing in thickness of the printed ink will increase the tendency of fracturing area occurred. Second factor is the type of substrate used. Substrate that is non-stretchable but flexible such as paper function better compared to materials like Lycra that can stretch in various dimensions. For this type of conductive ink, the fast drying is at room temperature for 5 – 15 minutes. The Bare Conductive Electric Paint will have bad effect for both physical and electrical performance if they are exposed to certain limit of high temperature. The typical properties of the bare conductive ink are summarized as in Table 3.1.

Figure 3.2: Carbon Black Bare Conductive Ink (Notes, 2015)

Table 3.1: Typical Properties of CB Bare Conductive Ink (Notes, 2015)

Colour	Black
Viscosity	Highly viscous and shear sensitive
Density	1.16 g/ml
Sheet Resistance	55 Ω/sq @ 50 microns or 32 Ω/sq when using brush
Operation Based	Water-based
Used by	6 months after opening
Curing Temperature	Dry at room temperature for 5 – 15 minutes. The curing time can be reduced by placing the ink under low intensity heat source or warm lamp

3.2.2 Singlewalled Carbon Nanotubes (SWCNTs)

As stated before, there are two different type of conductive ink that has been used to complete this research. For the second types of conductive ink, the commercial singlewalled carbon nanotubes conductive ink was used for this research. The ink is solvent based conductive ink that has good adhesion properties and it is primarily formulated for Screen Printing Transparent Conductors. This ink includes of CNTs which is exhibit good conductivity and oxidation resistance. This version of conductive ink are also suitable to be used in printed and flexible electronics, thin film resistors, photovoltaic and electrochemical sensors. The properties of the SWCNTs are as shown in Table 3.2.

Table 3.2: Typical Properties for SWCNTs (Cart, 2012)

Colour	Black
Viscosity	Viscous liquid
Density	0.001 g/ml
Sheet Resistance	<1000 Ω/sq
Used by	12 months after opening
Storage Temperature	2 – 8 °C
Curing Temperature	Dry at 100 °C using oven for 1 minutes

3.3 Sample Preparation

The sample preparation became one of the most crucial process for this research because the printing techniques also influence the thermal and mechanical properties for both inks. For this study, the sample were prepared by using manual printed method instead of screen printing techniques. It is because of CB conductive ink is not compatible with the screen printing technique. The standard size of the stencil screen-printing is not acceptable for the both ink in order to produce a better result. Thus, manual printed method by using cellophane tape as the screen printed medium is the best way to overcome this problem. For both inks, most of the sample preparations were same exclude for the curing part. The samples were prepared by following few steps as listed below:

1. Since the CB and SWCNTs conductive ink were printed on TPUs by using manual printing method. Hence, for the beginning process, the TPUs substrates were measured and marked as the dimension stated in Table 3.3. Next, the cellophane tape is placed on the marked point to form the screen frame as in Figure 3.3. During conduct this step, ensured that the layer of the cellophane tape and the width of the

screen frame followed the dimension since different width and thickness will affect the Rs of the ink.

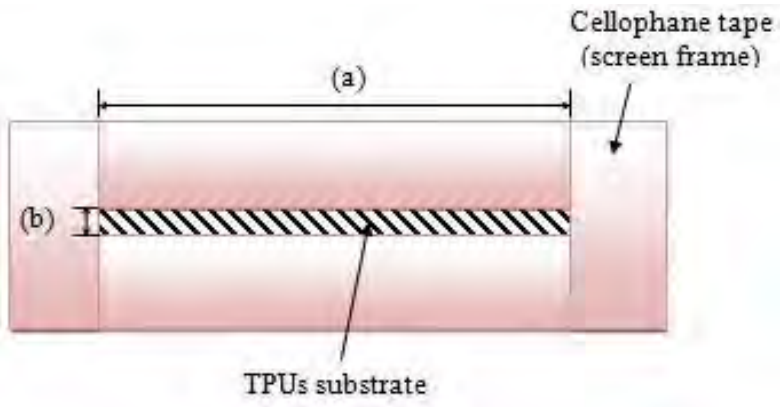

Figure 3.3: Top View of Screen Frame Printing

Table 3.3: Screen Frame Dimensions

(a) Length	30 mm
(b) Width	3 mm

2. Small amount of conductive inks were put on the top of the screen frame. Then, the ink is spread follow the screen frame with the low pressure and gently moves by using razor blade. The razor blades was moved toward the other end of screen frame in one direction and keep repeated the step until the ink distributed uniformly and fully covered the TPUs surface. The illustration of the screen printing process is presented in Figure 3.4 and Figure 3.5 below. Next, for further understanding, the sample of the completed printing process is illustrated as in Figure 3.6.

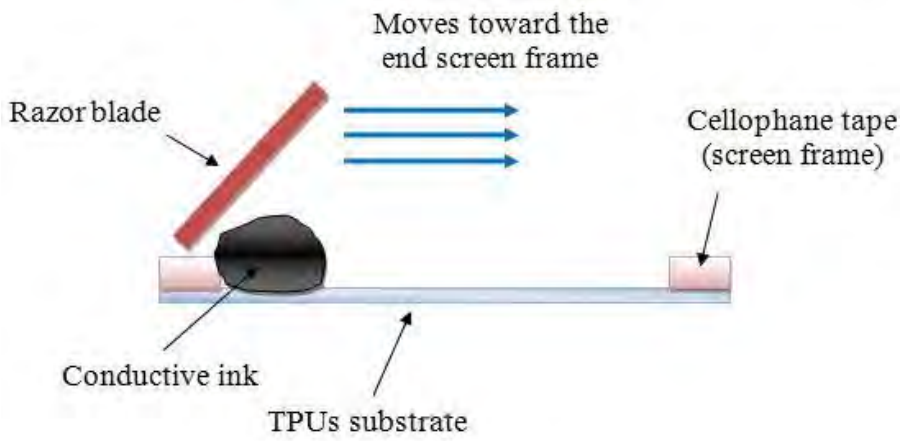

Figure 3.4: The Illustration of the Screen Printing Process from Side View

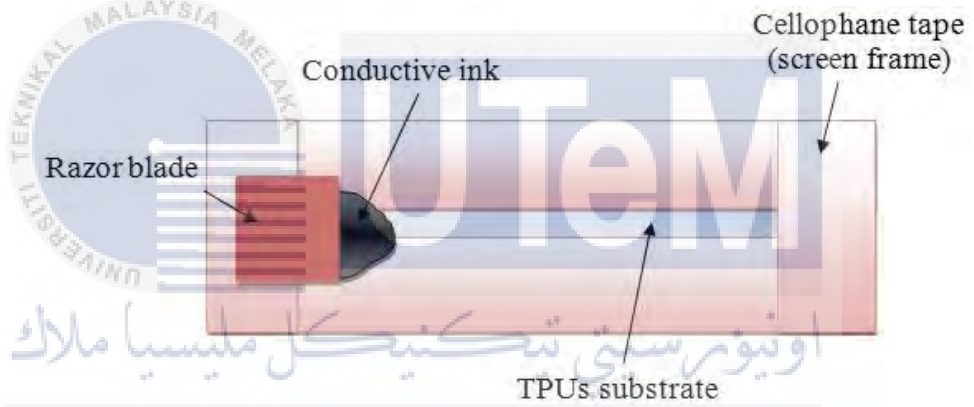

Figure 3.5: The Illustration of the Screen Printing Process from Top View

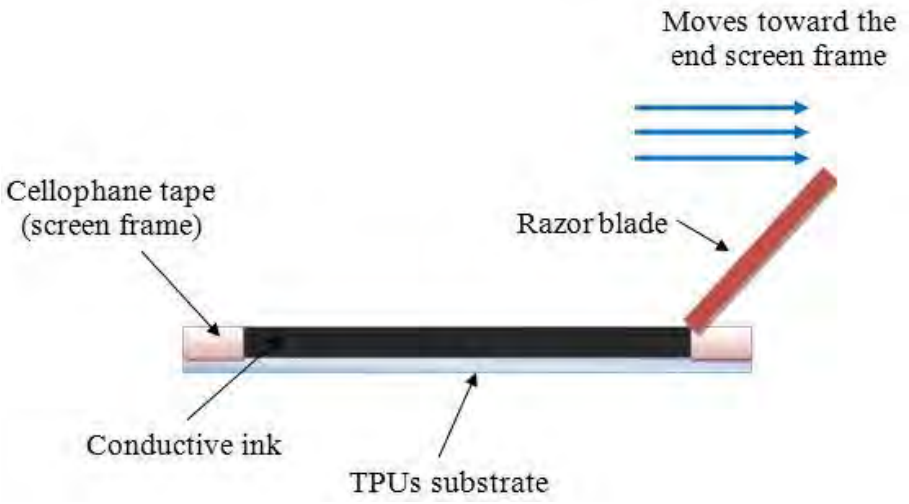

Figure 3.6: Side View for the Completed Printed Sample

3. Then, the samples were cured at different conditions followed the data sheet provided. For carbon black conductive ink, the samples were cured at room temperature for 5 – 15 minutes while for the SWCNTs conductive inks, the samples were cured by using oven. The oven was set up at temperature 100 °C for 1 minutes. Figure 3.7 below shows the oven that has been used to cure the SWCNTs conductive ink during this research.

Figure 3.7: Oven Used for Curing Process of SWCNTs

4. For accurate result purpose, the samples were divided into five sections as shown in Figure 3.8 below. Next, at each point, three reading were taken to get average value of sheet resistance. The sample's dimension were set up as shown in figure below where 30 mm length and 20 mm width for substrate. Next, the marked points include of 20 mm length and each point comprised of 4 mm in length. For the printed conductive ink, the width is 3 mm while the thickness is 0.08 mm.

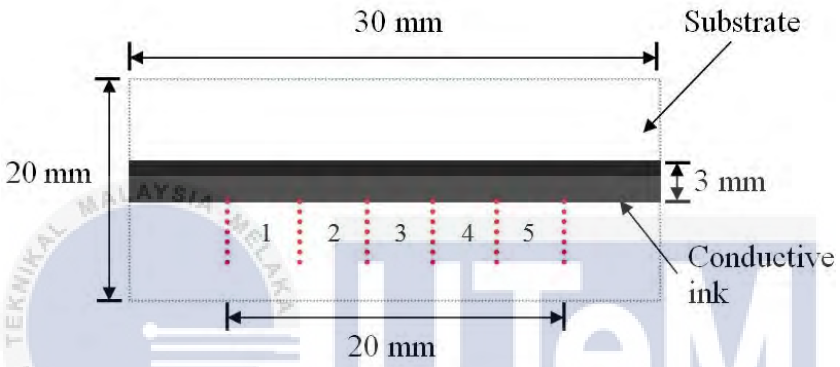

Figure 3.8: Top View of Marked Sample

3.4 Experimental

3.4.1 SEM Analysis

Scanning Electron Microscope (SEM) analysis was conducted to investigate the weight fraction and distribution of the filler particles in both CB and SWCNTs conductive inks. This part is very important since both of ink are ready made and both concentrations were totally different as stated in data sheet (Appendix C1 and Appendix C2). SEM analysis was conducted onto both samples before the samples were exposed to the thermal and mechanical test. By performed this analysis, the data of weight percent and atomic percent for both conductive inks were collected.

Figure 3.9: Scanning Electron Microscope (SEM)

3.4.2 Sheet Resistance under Room Temperature

For the case I, the samples were measured without any external thermal and mechanical force applied, which is sheet resistance, measured at room temperature, 32 °C. The data of this case important as the base data and the data also have been compared with the data excluded in the data sheet provided for both inks, refer Appendix C1 and Appendix C2. This cases is the simplest case since it is not involved others equipment such as thermal imaging analyzer, hair dryer to supply heat and vernier calliper as the stretchable jig. The sheet resistance of both samples were measured by using four-point probe system as shown in Figure 3.10 and 3.11. The data were collected as displayed in computer.

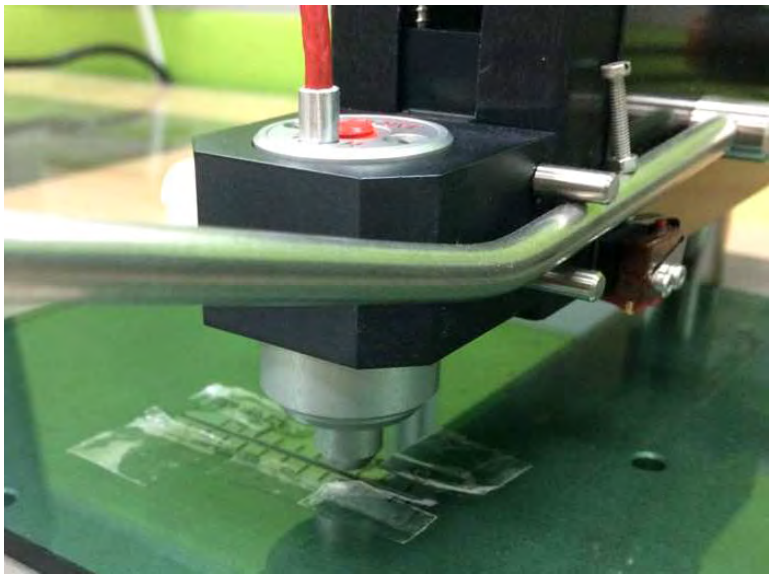

Figure 3.10: Sheet Resistance Measured at Room Temperature

Figure 3.11: Illustration for Measuring Sheet Resistance Technique

3.4.3 Sheet Resistance under Designed Temperature

Case II involved of measuring sheet resistance under heat applied at 40 °C, 60 °C and 100 °C. As shown in Figure 3.12, hair dryer has been used as the heater on this research. The hair dryer has three levels of heating which are low, medium and high levels. The reason of hair dryer was chosen as the equipment used to supply heat are the levels of heating are easy to set up and the equipment easy to handle. Next, in order to ensure that the heat supply was not less or exceed than the temperature designed, thermal imaging analyzer was used to control the heat supply.

For this case, the samples for both inks, which are CB and SWCNTs, are exposed to the three different temperatures. As mention before, the temperature includes of 40 °C, 60 °C and 100 °C. To get a more data, Rs were measured before the samples exposed to the designed temperature. From this step, the reduction values of sheet resistance after heat applied were calculated. The Rs was measured by using four-point probe system. As stated at the experimental set up, the samples for both inks were divided into five points and three times of reading were taken at each point to get the average data. The data from this experiment was recorded and have been discussed on the discussion section. For more understanding about the experimental set up, it has been illustrated from the top view as in Figure 3.13.

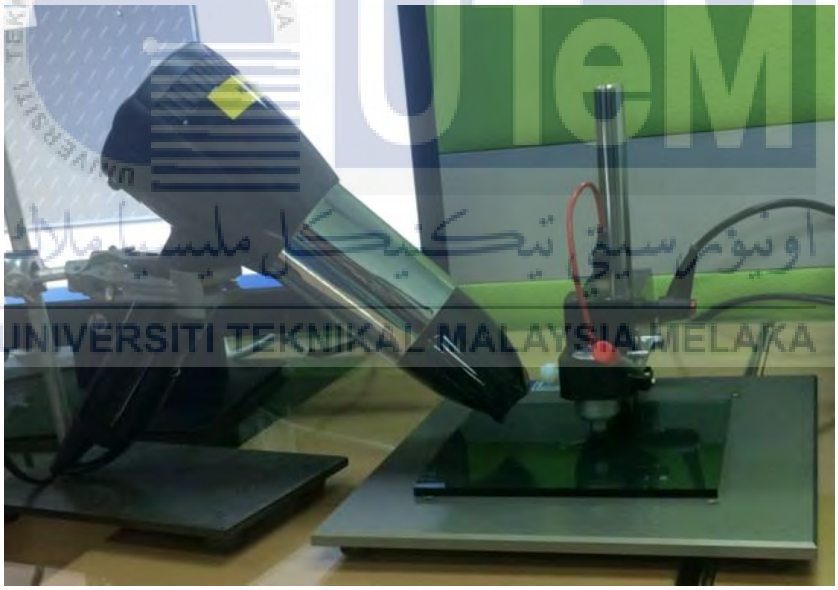

Figure 3.12: Front View of Experiment Set Up for Sheet Resistance at Designed Temperature

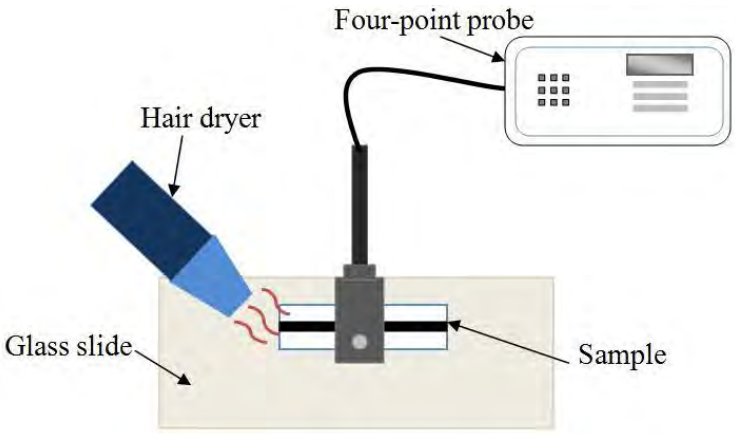

Figure 3.13: Top View of Experiment Set Up for Sheet Resistance at Designed Temperature

Figure 3.15 below shows the example of image that captured during the experiment for temperature 100 °C that is taken by using thermal imaging analyzer as in Figure 3.14. From the figure, it shows that the ink contain almost 100 °C of temperature. Same step were repeated for temperature 40 °C and 60 °C.

Figure 3.14: Thermal Imaging Analyzer Used

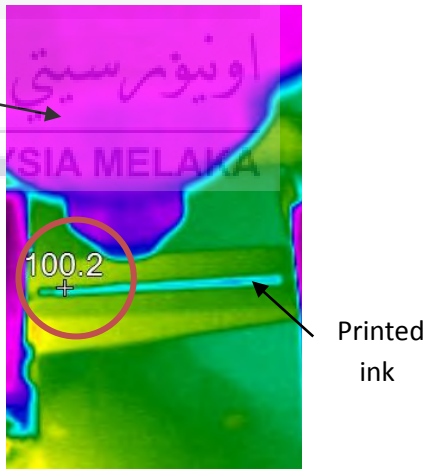

Figure 3.15: Image Captured by Thermal Imaging Analyzer for Temperature 100 °C

3.4.4 Sheet Resistance under Strain

For this experiment, which is case III, the correlation between sheet resistance and strain for each samples of the conductive ink are required to be investigated. Each sample were stretched by manual method and the vernier callipers are used as the tools to stretch the samples as illustrated in Figure 3.16. In room temperature, all samples were stretched at four different levels of strain. The strain level were control in percentage value, which are strain at 20 %, 40 %, 60 % and 80 % of elongation. Metal binder clips and double tape were used to attach and clip the samples at the lower jar of the calliper. Next, the lower jar of the calliper was pulled to the right for apply strain to the samples. Figure 3.17 shows the technique of sample attached to the vernier calliper.

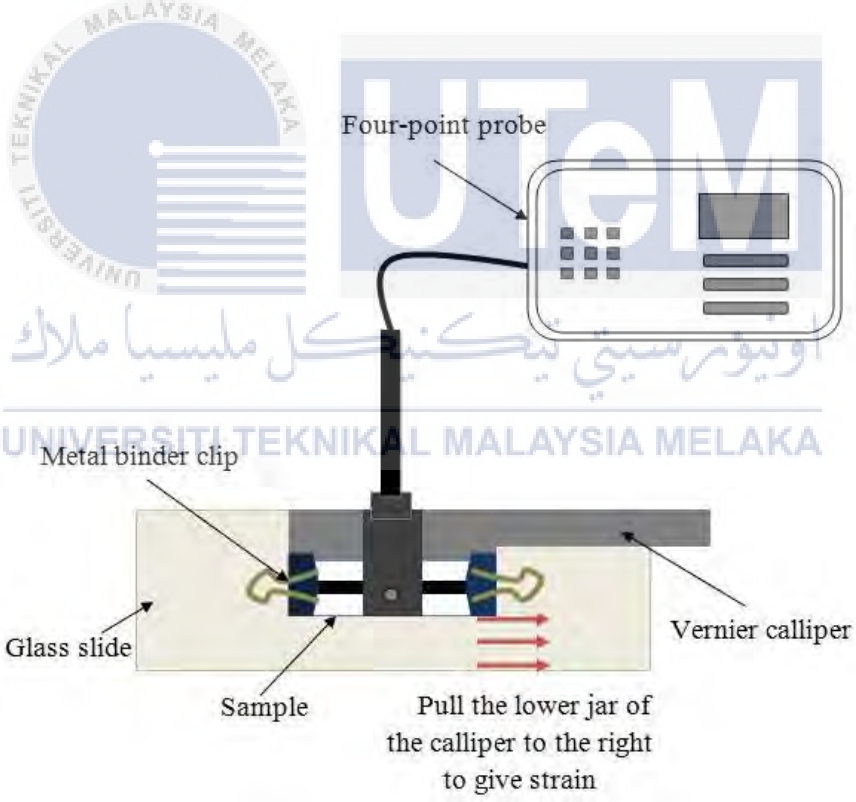

Figure 3.16: Top View of Experiment Set Up for Sheet Resistance under Strain

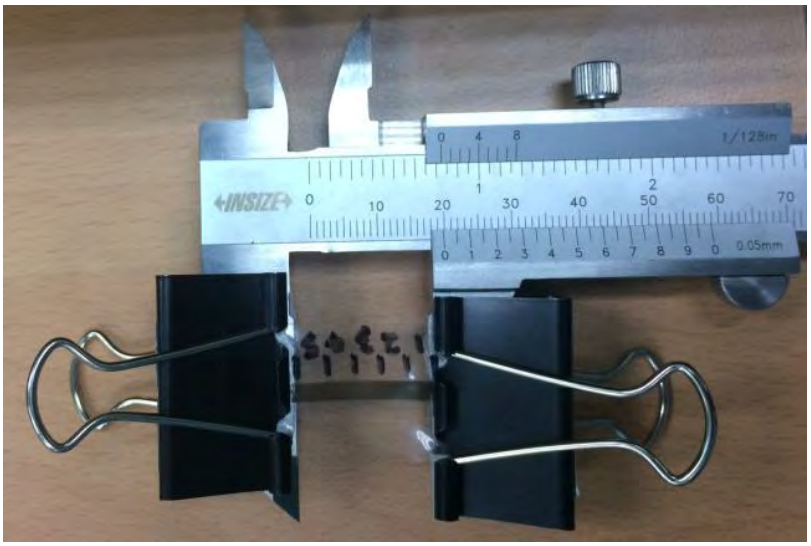

Figure 3.17: Top View of Clipped Sample at the Vernier Calliper

As stated in the experimental set up, the initial length of the marked point conductive ink is 20 mm. The samples were stretched until achieve the percent of elongation as circled in Figure 3.18 and Figure 3.19 below. In order to calculate the percent of increment Rs value, the measurement of Rs value before and after the strain applied was taken. The sheet resistance were measured three times at each five points to get the average data. The results of this experiment were summarized and have been discussed at the discussion section.

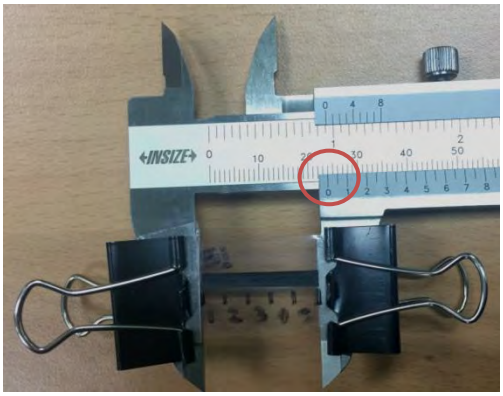

(a) 20 % of elongation, length 24 mm

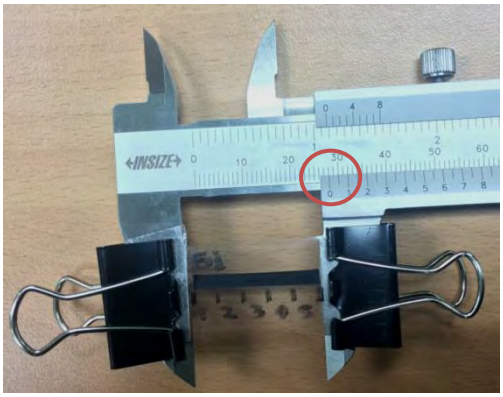

(b) 40 % of elongation, length 28 mm

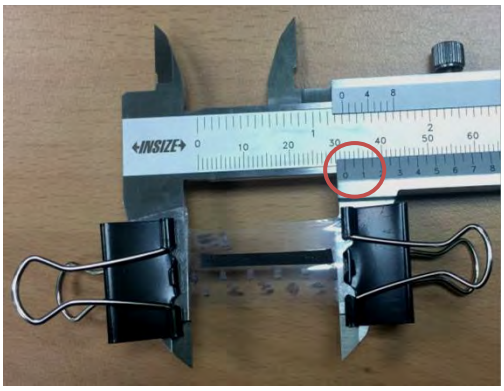

(c) 60 % of elongation, length 32 mm

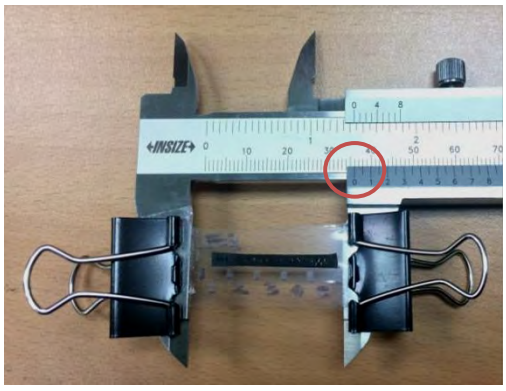

(d) 80 % of elongation, length 36 mm

Figure 3.18: Carbon Black Stretched Samples

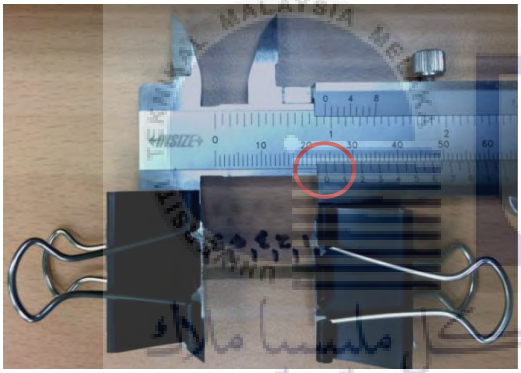

(a) 20 % of elongation, length 24 mm

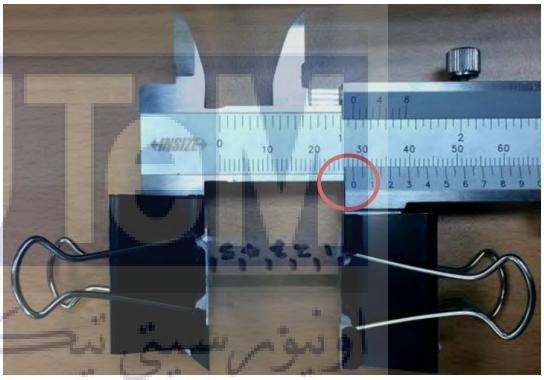

(b) 40 % of elongation, length 28 mm

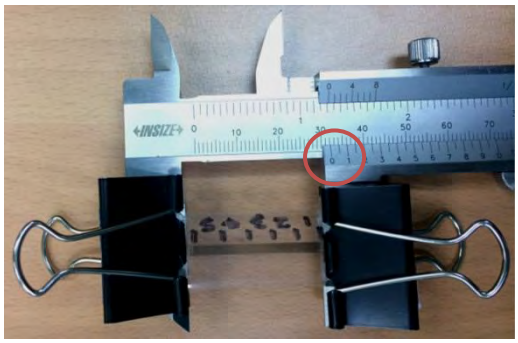

(c) 60 % of elongation, length 32 mm

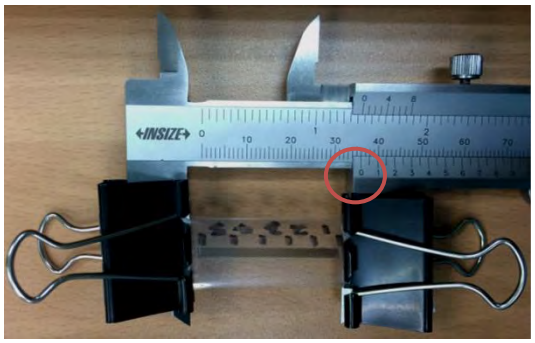

(d) 80 % of elongation, length 36 mm

Figure 3.19: Singlewalled Carbon Nanotubes Stretched Samples

CHAPTER 4

RESULT AND DISCUSSION

4.1 Introduction

For this research, readymade polymer-based electrically conductive inks, which are carbon black and singlewalled carbon nanotubes, have been used to study the thermal and mechanical effect on sheet resistance. In the conductive inks, conductive path is one of the significant factors that will contribute to the good conductance materials. Thus, to produce the conductive path, it is important to have the higher filler or conductive particles in the inks. The bulk conductivity's magnitude will encourage the number of particles in making a metal like conductive path. In other words, highly structured filler results better conductivity of materials (Chung et al., 1982). Hence, the correlation between weight percentage of fillers and sheet resistance have been studied and discussed further in this section. Next, the qualitative analysis has been done by using Scanning Electron Microscopy (SEM) to study the morphology surface of the inks.

The thermal and mechanical test includes of three different cases. As mentioned in Chapter 3, the experimental set up comprised of the study on effect of sheet resistance at room temperature, designed temperature and strain applied. For the case II, which is designed temperature, hair dryer used to supply heat and thermal imaging camera used to control the applied heat. The heat applied includes of temperature at 40 °C, 60 °C and 100 °C. Next, for the case III, vernier calliper has been used as tools that applied strain to the samples. The strain includes of 20 %, 40 %, 60 % and 80 % of elongation.

4.2 SEM Analysis for Carbon Black and Singlewalled Carbon Nanotubes

By referring Appendix C1 and C2, which is the data sheet for CB and SWCNTs, it is stated that both inks have different properties for example in term of concentration. The concentration of CB is 1.16 g/ml where for the SWCNTs is 0.001 g/ml. The data sheets also mentioned that the viscosity for CB is high. Hence, in order to study the differences in term of the weight percentages of filler, both inks have been analyzed by using SEM analyzer.

4.2.1 Carbon Black's SEM Analysis

Figure 4.1 shows the results of SEM micrograph and element analysis for carbon black surface before applied thermal and mechanical effects. The result presents in the Table 4.1 summarized that CB contains 92.89 weight percentage of fillers for spectrum 1 and 82.75 weight percentage of fillers for spectrum 2. Both spectrum comprised of almost 100 wt.% of filler loadings. The higher value of wt.% of filler loadings resulted better conductivity or in other words, it will produced material that has lower sheet resistance.

(a)

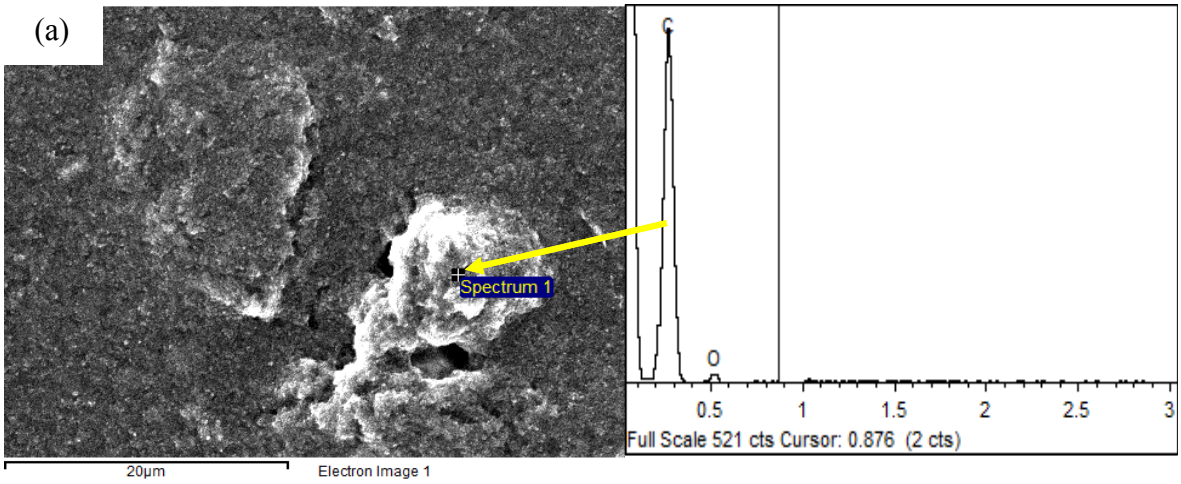

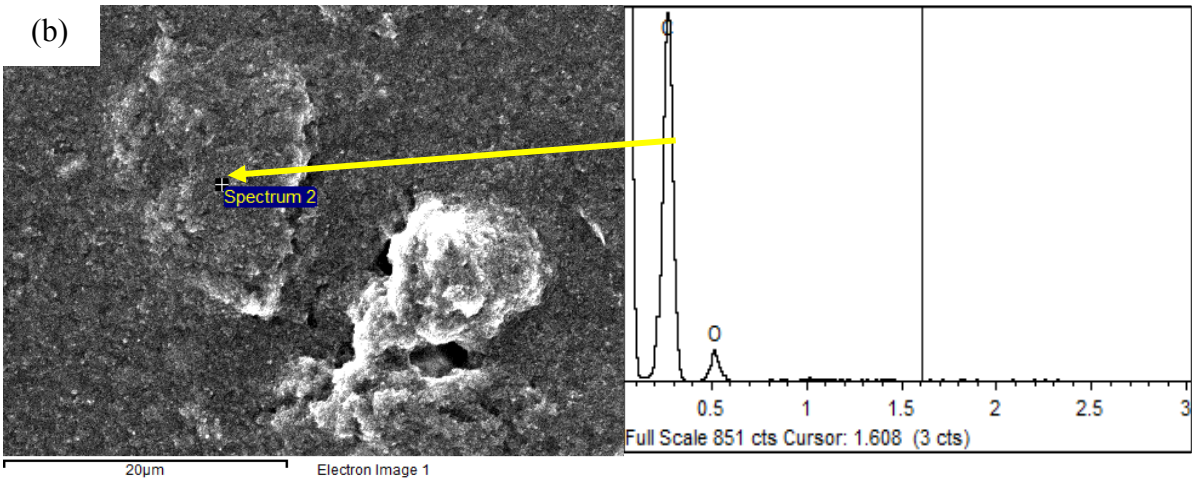

Figure 4.1: SEM Micrograph and Element Analysis for Carbon Black Surface
(a) Spectrum 1 (b) Spectrum 2

Table 4.1: Elemental Composition for CB

Spectrum	Element	Weight (%)
1	Carbon (filler)	92.89
	Oxygen	7.11
2	Carbon (filler)	82.75
	Oxygen	17.25

4.2.2 Singlewalled Carbon Nanotube's SEM Analysis

This section is describing about the result of SEM micrograph and element analysis for SWCNTs surface at room temperature as shown in Figure 4.2. The analysis was conducted before the samples were exposed to the thermal and mechanical effect. From the Figure 4.2, the graphs show the presence of other element, which are magnesium, Mg and silicon, Si. The samples also comprised of carbon elements. However, the presence of carbon elements in SWCNTs is lower than CB which are 43.41 wt.% and 51.66 wt.% of filler loading for spectrum 1 and 2.

Next, by referring Table 4.2, it shows that this samples contained of 7.51 wt.% of Mg and 11.60 wt.% of Si for spectrum 1 while 6.37 wt.% of Mg and 8.87 wt.% of Si for spectrum 2. Magnesium and Silica contributed to the increase in hardness of material in term of stretchability and flexibility. Si elements will improve the ink adhesion properties since it has large surface area and acts as binder that is good in print quality (Svanholm, 2007). Binder also used as the elements to make the filler particles stick to the TPUs substrate and to increase the attraction between conductive filler particles (Banfield, 2000).

(a)

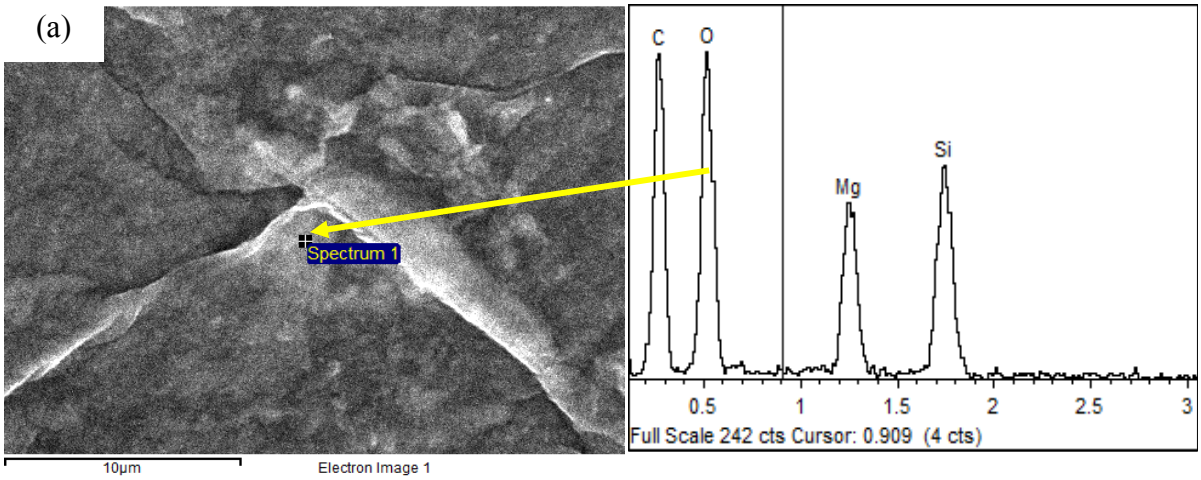

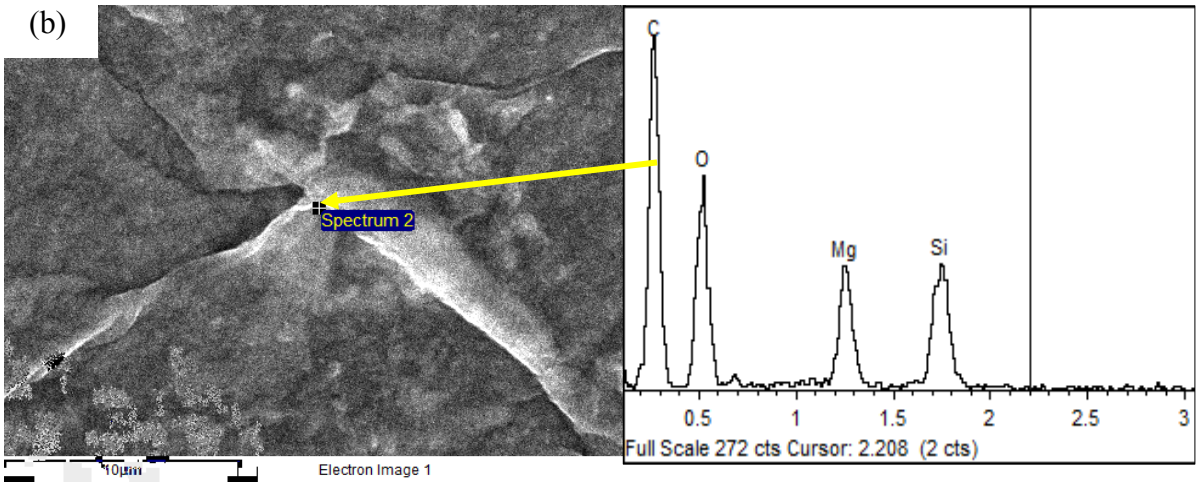

Figure 4.2: SEM Micrograph and Element Analysis for SWCNTs Surface (a) Spectrum 1 (b) Spectrum 2

Table 4.2: Elemental Composition for SWCNTs

Spectrum	Element	Weight (%)
1	Carbon (filler)	43.41
	Oxygen	37.48
	Magnesium	7.51
	Silica	11.60
2	Carbon (filler)	51.66
	Oxygen	33.10
	Magnesium	6.37
	Silica	8.87

4.3 Case I: Sheet Resistance under Room Temperature

Case I includes of measuring sheet resistance of the samples at room temperature without exposed to the thermal and mechanical test. The results below is the average data calculated from the four-point probe system. Based on the results obtained in Figure 4.3, the average sheet resistance for CB sample that was exposed to the room temperature is 90.57 Ω/sq while for the SWCNTs sample is 505 Ω/sq. By referring data sheet for both ink, Appendix C1 and Appendix C2, it is stated that the sheet resistance value for CB black at room temperature should be lower than 55 Ω/sq. The results obtained for CB sheet resistance is higher than the value stated in the data sheet because of the screen printing technique, which is the dimension of the printed ink, is not suitable with the CB recommended printing.

Next, for the SWCNTs samples, the sheet resistance value stated in data sheet is should be lower than 1000 Ω/sq. As stated in previous section, carbon black contains higher weight percentage of filler loading compared to singlewalled carbon nanotubes. Thus, CB samples has lower value of sheet resistance compared to SWCNTs (Dziedzic et al., 1993). At high weight percentage of fillers, a large decrease in sheet resistance value of polymer-based conductive ink can be related to the transference of the large number of charged particles through the continuous conductive network form. In other words, the level of conductivity increase due to the continuous network of conductive paths that have been developed in the polymer matrix (Hasnaoui et al., 2011). Next, the sheet resistance also decreasing as the filler content reaches the electrical percolation threshold.

Similarly, as the increase in filler loading, the conductive paths continuously formed by filler particles that contact and come closer to each other, which charged species, can move across particles to particles under electric fields. This phenomenon shows the stable electrical conductivity occurs. Polymer-based electrically conductive ink

is strongly depends on the fillers loading. The higher the fillers loading contains in the polymer-based conductive ink, the resistivity at some area also will decrease (Sau et al., 1998).

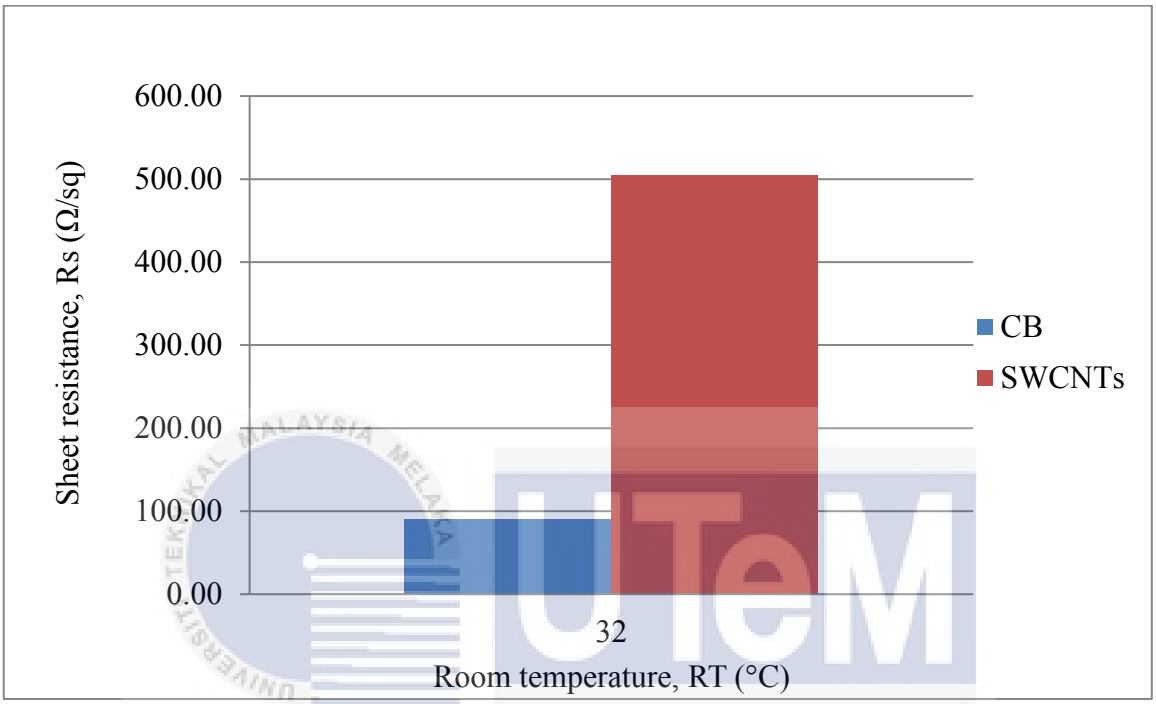

Figure 4.3: Bar Chart for Rs of CB and SWCNTs at Room Temperature

4.4 Case II: Sheet Resistance under Designed Temperature

For this case, the sheet resistance is measured under thermal effects where the heat is applied by using hair dryer. The samples for both inks were exposed to the four different level of temperature, which are temperature at 32 °C, 40 °C, 60 °C and 100 °C. Based on the result obtain from Figure 4.4, it shows the result for average of sheet resistance for carbon black versus designed temperature. The bar charts contains the data for sheet resistance before and after the samples were exposed to the heat. These data is important to calculate the percent reduction of the sheet resistance after the samples were exposed to heat by using equation 4.1 as stated.

$$\%\ of\ reduction = \frac{Rs\ after\ heated - Rs\ before\ heated}{Rs\ before\ hetaed} \quad (4.1)$$

Based on the results obtained in Figure 4.4, the average sheet resistance for CB sample that has been exposed to the room temperature, 32 °C was 90.57 Ω/sq. Next, before the samples is exposed to the heat, the value of sheet resistance was 85.01 Ω/sq and dropped to the 81.87 Ω/sq after temperature 40 °C is applied to the samples. For temperature 60 °C, the value of sheet resistance obtained before heated was 86.77 Ω/sq and decreased to the 68.61 Ω/sq. However, for the samples that has been exposed to the 100 °C, the results shows that the values of sheet resistance after heated decrease half from the initial value which are 85.11 Ω/sq dropped to 40.43 Ω/sq.

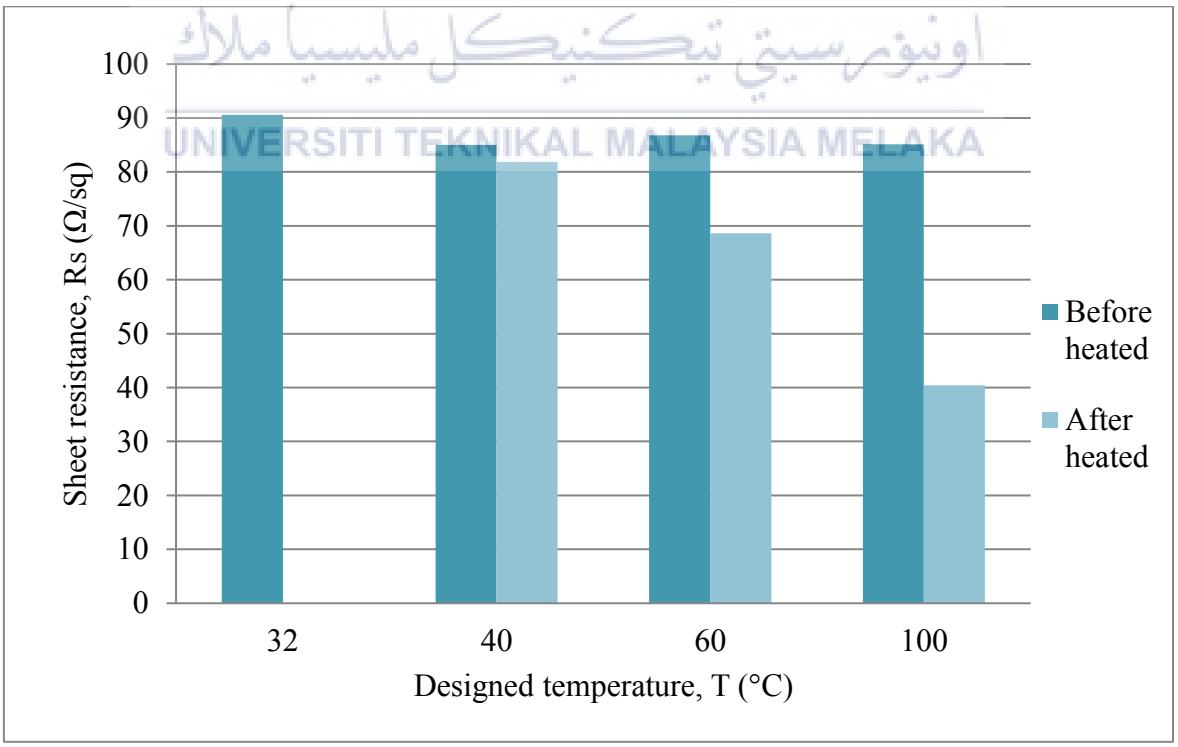

Figure 4.4: Bar Chart for Sheet Resistance of CB versus Designed Temperature

The bar chart in Figure 4.5 shows the results for average of sheet resistance for singlewalled carbon nanotubes versus designed temperature. The results also contains of data obtained for before and after heated in order to calculate the value of sheet resistance in percent reduction. The bar chart shows the value of the average sheet decreases with increasing temperature. The average sheet resistance for SWCNTs sample at room temperature, 32 °C was 505 Ω/sq. For temperature 40 °C, the value of sheet resistance obtained before heated was 782.76 Ω/sq and dropped to the 739.2 Ω/sq. Next, before the samples is exposed to the heat, the value of sheet resistance was 683.68 Ω/sq and dropped to the 608.98 Ω/sq after temperature 60 °C is applied to the samples. Lastly, for the highest level of temperature which is 100 °C, the value sheet resistance before heated is 1089.83 Ω/sq and reduced to 825.34 Ω/sq.

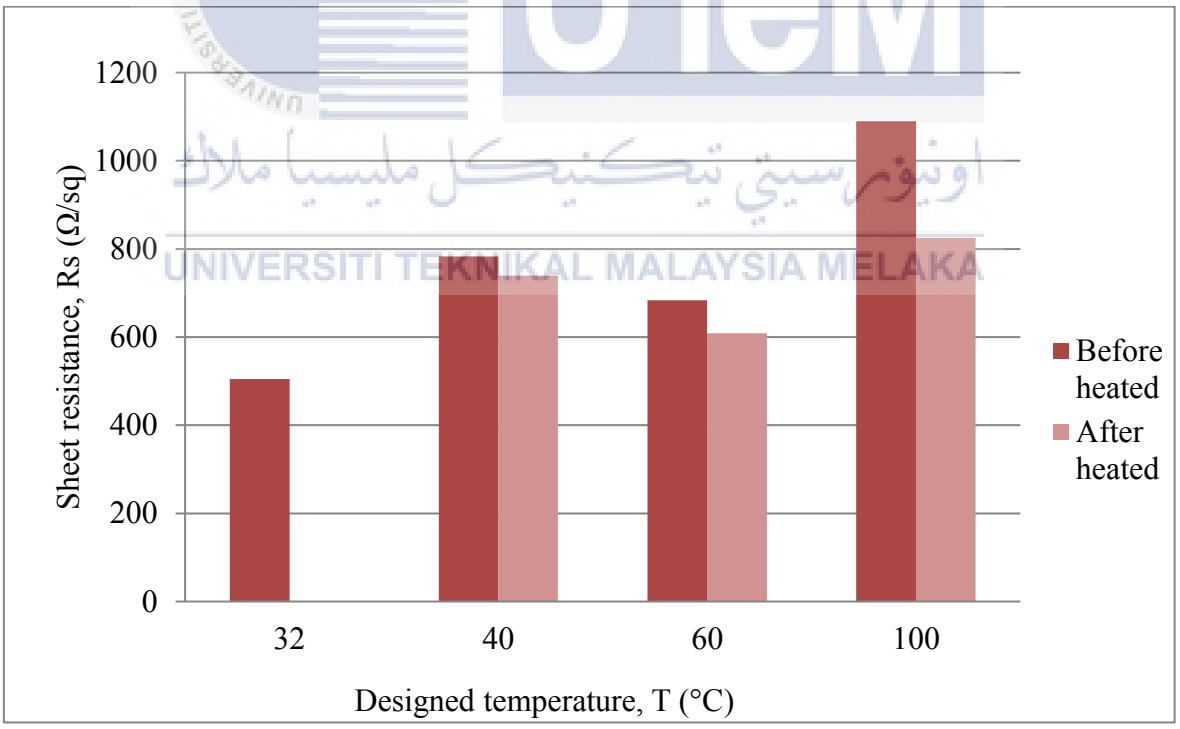

Figure 4.5: Bar Chart for Sheet Resistance of SWCNTs versus Designed Temperature

By referring Figure 4.6 and Figure 4.7, the graph displays the result of average sheet resistance in percent reduction for CB and SWCNTs inks after heat applied against design temperature. By using Equation 4.1 as stated in previous section, the percent reduction of average Rs is calculated. For carbon black conductive ink, the Rs reduction at 40 °C is 4 %, 21 % of reduction for temperature 60 °C and 52 % of reduction for 100 °C. Meanwhile, for the singlewalled carbon nanotubes, the percent reduction of average sheet resistance value at 40 °C is 6 % and 11 % of reduction for temperature 60 °C. Finally, for the highest level of temperature, which is 100 °C, the reduction is 24 %.

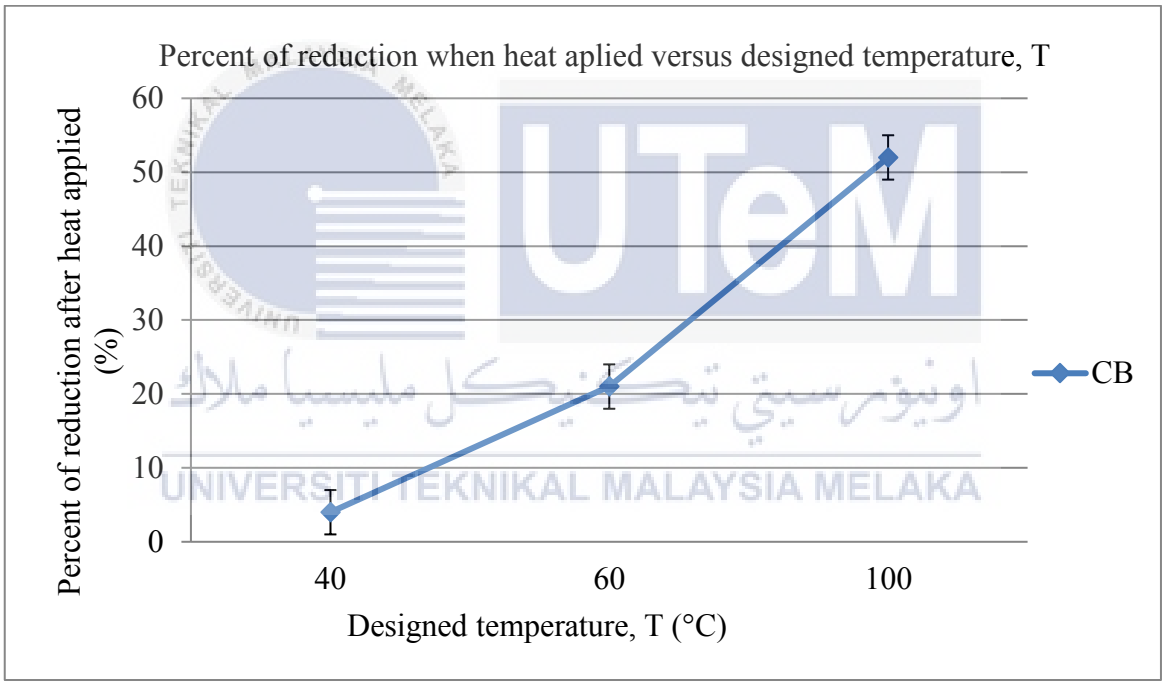

Figure 4.6: Graph of Sheet Resistance in Percent Reduction for CB Ink after Heat Applied versus Design Temperature

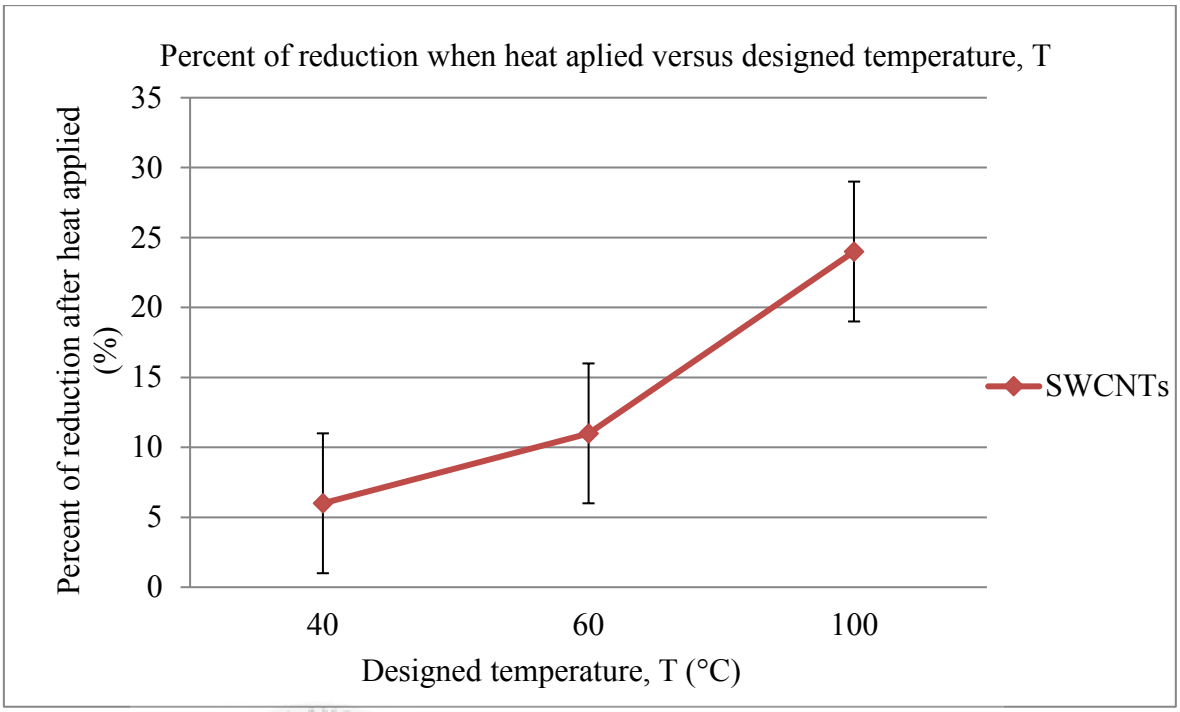

Figure 4.7: Graph of Sheet Resistance in Percent Reduction for SWCNTs Ink after Heat Applied versus Design Temperature

Generally, based on the results, it shows that the percent reduction of average sheet resistance is increase as the temperature applied increase. Since CB contains more filler loading as been mentioned in previous section, hence the percent reduction for CB samples is higher compared to SWCNTs sample. Higher filler loading will contribute to the increasing number of conductive networks. The conductive networks allowed electric current to pass across the filler particles (Oskouyi et al., 2014). Thus, Rs value decrease with the increase of conductive networks formed.

The decreasing of sheet resistance value shown by the graph is due to the thermal effect where each level of temperature increased results decreased in mass of printed conductive ink. In another words, it is decrease in polymer amount. Because of this, the resistivity is decrease due to the increasing in weight percentage of filler loading, as amount of the latter remain unchanged (Dziedzic et al., 1993). Next, increasing in temperature also gradually leading to make the fillers connected with each particles easier

and decrease the impedance. Decrease in impedance will results more energy that captured by the electrons and they would control the potential barrier easily (Li et al., 2009).

Increasing in temperature applied to the samples also lead to the increase of size particles. It will cause the conductive fillers particles expand and become closer to each other. Thus, it also reduced the gap between each particles and form a better conductive networks. This phenomenon makes the electron move across particles to particles easily conductive phase also increases (Dziedzic et al., 1993) . As result, the sheet resistance value decreased.

4.5 Case III: Sheet Resistance under Strain

It is important to understand the correlations between strain and sheet resistance since sheet resistance were also sensitive to the strain. Electrical properties of the conductive ink can be affected by strain applied. It is also depending on the type of conductive filler and weight percentage of filler loading (Das et al,. 2002). Thus, the relationship of the strain and the sheet resistance were discussed further in this section.

The graph in Figure 4.8 indicates the result for average of sheet resistance for CB conductive ink versus strain applied. It was clearly shown in the graph, the average of sheet resistance increases with increasing of strain applied. Initially, before the samples were applied to the strain, the value of the average sheet resistance was 143.63 Ω/sq and increased to the 174.39 Ω/sq after 20 % of strain applied. Next, the average sheet resistance rose to 178.98 Ω/sq at 40 % of strain and 272.07 Ω/sq at strain of 60 %. For the 80 % of strain, the value of sheet resistance increased to 307.17 Ω/sq that is increasing half from its initial value.

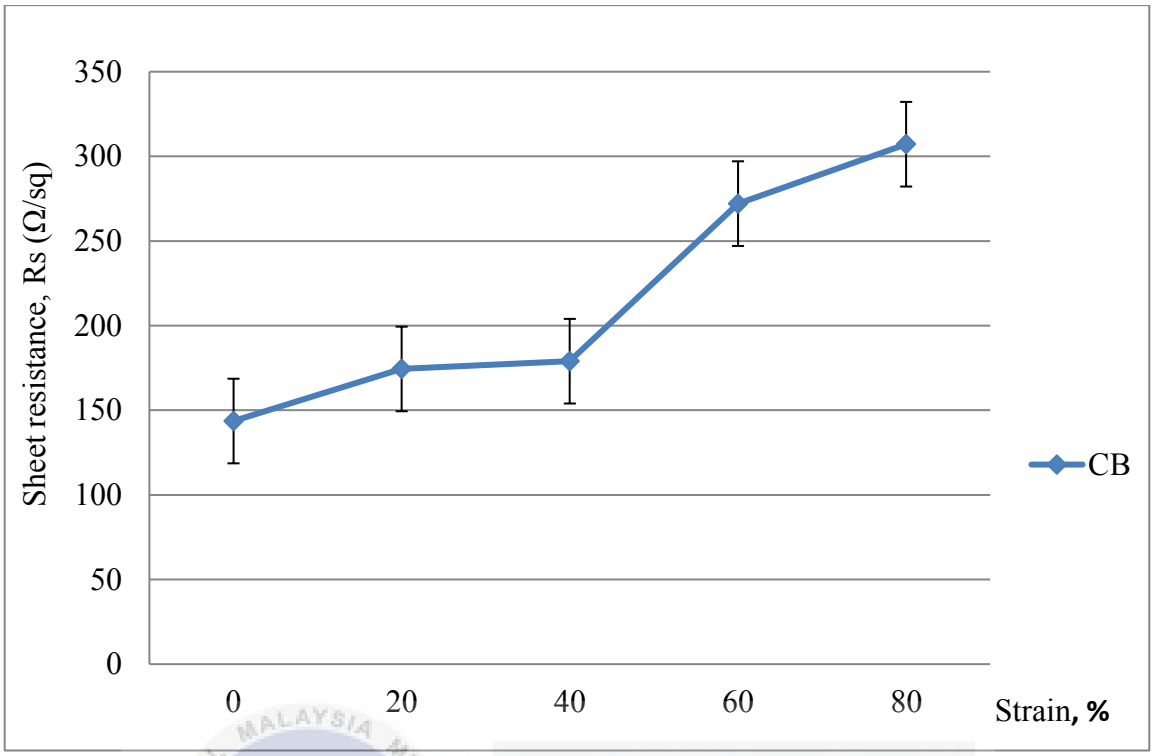

Figure 4.8: Graph of Sheet Resistance for CB versus Strain

Then, for the SWCNTs samples, the results were obtained and have been illustrated as in Figure 4.9. From the graph pattern, it shows that the average of sheet resistance is directly proportional to the strain applied. Therefore, higher strain applied resulted increasing in sheet resistance value. The average sheet resistance value were 598.59 Ω/sq at 0 % of strain, 666.22 Ω/sq at 20 % of strain and 904.74 Ω/sq at 40 % of strain. Next, the value was increased to 1293.18 Ω/sq at 60 % of strain. Lastly, for 80 % of strain, the average sheet resistance was 1606.39 Ω/sq. This experiment was not include 100 % of strain because of the larger cracking occurs to the printed samples and four-point probe was unable to measure the average sheet resistance value.

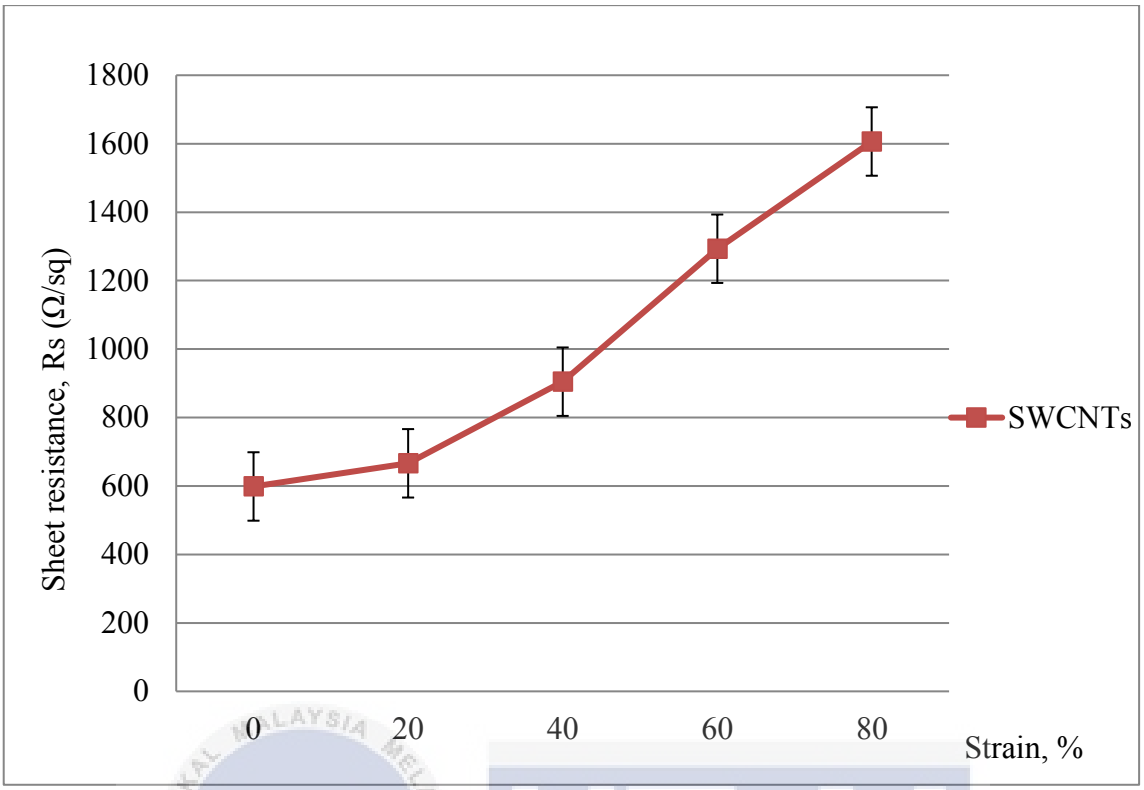

Figure 4.9: Graph of Sheet Resistance for SWCNTs versus Strain

Figure 4.10 displays the bar graph for the percent increment of average sheet resistance after strain applied at room temperature. Based on the results, the percent increment of average sheet resistance after strain applied for CB conductive ink is 114 % while for SWCNTs is 168 %. The percent of increment is calculated by using Equation 4.2. The percent of increment for SWCNTs sample is higher compared to CB samples. Generally, the strain applied cause the formation of gap between the filler particles. In another words, the strain applied might destroyed the conductive path (Flandin et al., 2000). As mentioned before, the conductive network is very important to allow the electron across through one particle to another particle. Thus, the situation will leads to the increasing in average of sheet resistance for both conductive ink.

$$\% \ of \ increment = \frac{Rs \ after \ applied \ strain - Rs \ before \ applied \ strain}{Rs \ before \ applied \ strain} \quad (4.2)$$

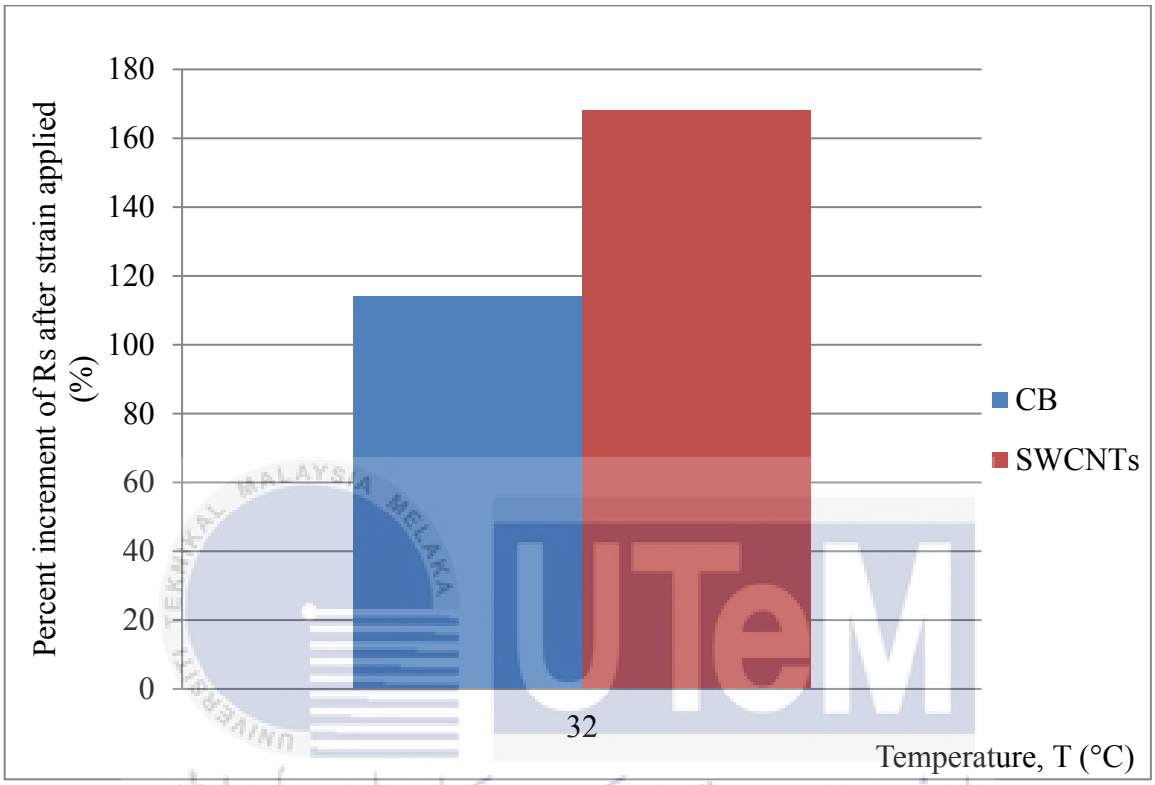

Figure 4.10: Graph of Sheet Resistance for SWCNTs versus Strain

Besides, this theory also has been discussed by Das et al., (2002), the research claimed that the increasing percent of strain will cause the space between each conductive fillers continually increase and breakdown of the existing conductive path occurs. Hence, the possibility of the tunnelling of electrons for electrical conductivity decreases. The CB samples has low percent increment of sheet resistance after strain applied compared to the SWCNTs sample is because of CB samples has higher filler loading. Thus, it will lead to a better aggregation tendency, which will control the breakdown of conductive networks. In another words, the damage occurs to the conductive path for CB samples is more lower

compared to SWCNTs samples. The breakdown of conductive networks for CB conductive ink also occurs in a slower rate due to the high filler loading contains in the ink.

Stretching of the conductive ink might cause two phenomenons, which are networks destruction and network formation. It is depends on the filler concentration and filler types. However, based on the results, it is clearly seen that the destruction of conductive networks were occurred instead of network formation since the increment of sheet resistance were keep increased over the strain applied (Sau et al., 1998). The breakage of the conductive networks occurs is caused by the increase in gap between particles. According to Pramanik et al., (1993), the electrons will contact in connect to each other when filler particles space is not more than few tenths of nanometres.

(a) 20 % of elongation (b) 40 % of elongation

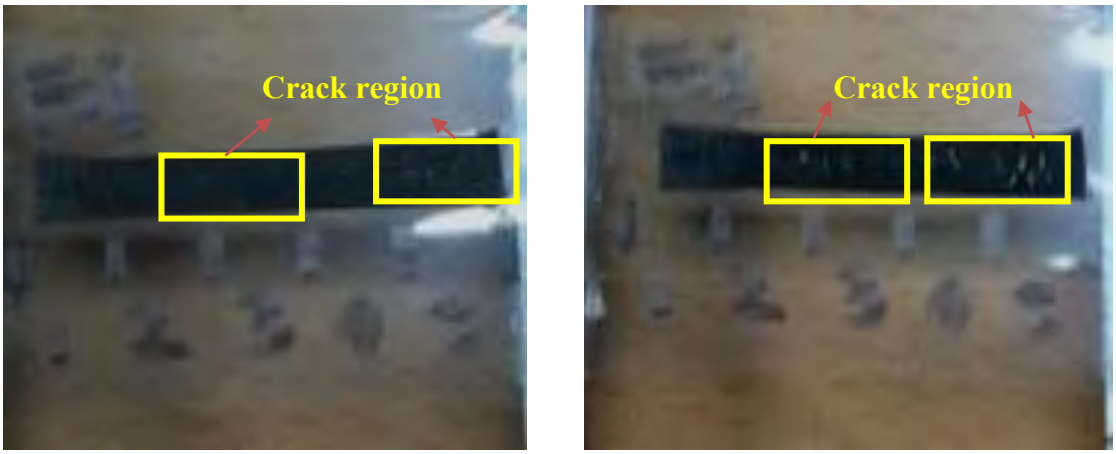

(c) 60 % of elongation (d) 80 % of elongation

Figure 4.11: Images of Stretched CB Samples

Figure 4.11 above shows the image for CB samples that were stretched at 20 %, 40 %, 60 % and 80 % of elongation. From the image, it can be seen that cracking start to occur at 60 % of strain and rapidly increase at 80 % of strain. Meanwhile, for the SWCNTs sample, the images after the sample were stretched are summarized as in Figure 4.12. From the images, there is no cracking occurs on the surface on the conductive inks. This is because SWCNTs conductive contain Mg and Si that contributes to better adhesion properties and increase in hardness, which is able to resist strain. Even though there was a larger crack area on the CB conductive ink, the percent increment of sheet resistance is lower than SWCNTs sample due to the high fillers loading contained in the CB conductive ink.

(a) 20 % of elongation

(b) 40 % of elongation

(c) 60 % of elongation

(d) 80 % of elongation

Figure 4.12: Images of Stretched SWCNTs Samples

CHAPTER 5

CONCLUSION AND RECOMMENDATIONS

5.1 Conclusion

In conclusion, the effects of temperature and strains on sheet resistance of carbon black and singlewalled carbon nanotubes conductive inks were investigated. Next, the correlations between weight percentage of filler loading and sheet resistance also were studied in this research. The experimental work was conducted in order to achieve the objectives of this research. All the results is obtained by using four-point probe system to measure the sheet resistance of the samples and Scanning Electron Microscope (SEM) to study the morphology surface of the conductive inks.

For the cases that related to the thermal effects, the results obtained shows that the sheet resistance was decreased as the temperature applied increases. This is due to the coefficient thermal expansion of the filler particles. The expansion in size of the conductive particles reduces the gap between each of particles. Lower gap between particles make the electron cross through each particles to the next particles easily then decreased the sheet resistance value. Next, the decreasing in gap between each of filler particles also contributes to the forming of conductive network paths.

As stated by many researches, SWCNTs should have better conductivity compared to CB since they contain nanoparticles filler that is smaller in size. Smaller in size of filler particles will leads to the better contact surface between the particles. Hence, it will create a better network of conductive paths. However, this research results shows that the CB has

better conductivity compared to SWCNTs. In another words, CB has lower sheet resistance value. This is caused by CB conductive ink has higher weight percentage of filler loading compared to SWCNTs as proved by SEM analysis.

Next, for the strain case study, the results obtained shows that the sheet resistance was increased when the samples exposed to the strain. This results was proved by both inks where there is a percent increment of sheet resistance value after strain applied to the samples. The stretching of samples caused the destruction to the conductive networks occurs and the breakage of the conductive networks also occurred. That is caused by the increase in gap between particles when the strain applied. The results for each case are summarized as in Table 5.1, Table 5.2 and Table 5.3 below. From the results that have been summarized in the tables below, it shows that weight of percentage filler loading plays major roles in this research. Next, weight of percentage filler loading also contribute to the good electrical properties of polymer-based conductive inks.

Table 5.1: Summary for Average Weight of Percentage Filler Loading for Both Inks

Type of Conductive Inks	Average wt.% of Filler Loading (%)
CB	87.82
SWCNTs	47.54

Table 5.2: Summary of Total Percent Increment of Rs after Applied Strain for Both Inks

Conductive Inks	Total Percent Increment of Rs After Applied Strain (%)
CB	114
SWCNTs	168

Table 5.3: Summary of Percent Reduction Rs after Applied Heat for Both Inks

Temperature (°C)	Percent Increment of Rs After Applied Heat (%)	
	CB	SWCNTs
32	0	0
40	4	6
60	21	11
100	52	24

5.2 Recommendations

Printed circuits that are both stretchable and flexible are highly demand in industry that can perform as better application. The difficulties to produce stretchable electronic with high quality while maintaining the electrical properties are the stretchable printed circuits must be able to expose with high level of temperature, able to have good adhesion properties, better in mechanical strength and low production cost. Hence, further investigation must be done in order to fulfil the customer requirement to have high quality of stretchable printed circuit. Next, stretchable printed circuit also will have valuable position in worldwide printed circuit markets.

In this research, several investigation that related to the thermal and mechanical effects on the sheet resistance have done by conducting experimental work. During conduct the experiment, there were some problems occurs and affecting the timeframe of the experiment. In order to overcome the problems, several actions must be taken for examples formulate the conductive ink by self instead of using readymade conductive ink. By formulating the conductive ink by self, the contents of the ink can be controlled easily

such as the weight percentage of the filler loading. It is difficult to discuss and comparing the value of sheet resistance for CB and SWCNTs conductive ink that have been used in this study since they are formulated with different concentrations. Next, they were also having different weight percentage of solvents and binder. Values of sheet resistance are strongly influenced by those items.

Besides, since both inks have different concentration of binder, hence the printing techniques must be changed from using stencil as the screen printing technique to the manual printing technique. Thus, it is very significant to know the weight percentage of binder and their viscosity. The adhesive strength of the ink is important because it can affect the sheet resistance since this study was related to the thermal and mechanical effects. The compatibility of both inks with the TPUs substrates is totally different due to the different formulation in term of adhesion properties. Because of this, the experiment must be done for several times in order to know the dimensions of the printed ink that compatible with the substrates.

Second recommendation is improve the curing method as it also play significant role in this study and ensure that the filler of the conductive inks distributed evenly during printing process. From observation during the experiment, the area that has lower filler loading resulted high value of sheet resistance. Thus, ensure that the ink is stirred before conduct the printing process. Lastly, further research on curing method, effects weight percentage of filler loading on Rs, effect of strains on Rs, how thermal affected Rs of conductive ink and fillers behaviour could be done as they plays major role in determining the electrical conductivity of polymer-based conductive ink.

REFERENCES

A guide to thermoplastic polyurethanes (TPU). (n.d.).

Agar, J. C. (2011). Highly Conductive Stretchable Electrically Conductive Composites For Electronic And Radio Frequency Devices By Highly Conductive Stretchable Electrically Conductive Composites For Electronic And Radio, (August).

All Leaflet.Pdf. (n.d.).

Banfield, D. (2000). Understanding and Measuring Electrical Resistivity in Conductive Ink and Adhesives. *Sgia*, 8.

Bautista, K. (2004). Four-Point Probe Operation Four-Point Probe Operation. *Film*, 1–8.

Cargill, M., Ireland, J. S., Bolk, S., Roxbury, W., Us, M. A., & Mccarthy, J. J. (2004). (12) United States Patent, *1*(12). https://doi.org/10.1016/j.(73)

Cart, a D. D. T. O. (2012). Price and Availability. *Reproduction*, (I), 16–18.

Chan, J., & Friedberg, P. (2002). Four-point probe manual. *EECS 143 Microfabrication Technology*, 1–3. https://doi.org/10.1002/j.1538-7305.1958.tb03883.x

Che, J., Çagin, T., & Goddard, W. A. (2000). Thermal conductivity of carbon nanotubes. *Nanotechnology*, *11*(2), 65–69. https://doi.org/10.1088/0957-4484/11/2/305

Chung, K. T., Sabo, A., & Pica, A. P. (1982). Electrical permittivity and conductivity of carbon black-polyvinyl chloride composites. *Journal of Applied Physics*, *53*(10), 6867–6879. https://doi.org/10.1063/1.330027

Das, N. C., Chaki, T. K., & Khastgir, D. (2002). Effect of axial stretching on electrical resistivity of short carbon fibre and carbon black filled conductive rubber composites. *Polymer International*, *51*(2), 156–163. https://doi.org/10.1002/pi.811

Dziedzic, A., Czarczyńska, H., Licznerski, B. W., & Rangelov, I. (1993). Further examinations of carbon/polyesterimide thick-film resistors. *Journal of Materials Science: Materials in Electronics*, *4*(3), 233–240. https://doi.org/10.1007/BF00224747

El Hasnaoui, M., Graça, M. P. F., Achour, M. E., Costa, L. C., Lahjomri, F., Outzourhit, A., & Oueriagli, A. (2011). Electrical properties of carbon black/ copolymer composites above and below the melting temperature. *Journal of Materials and Environmental Science*, *2*(1), 1–6. https://doi.org/10.4161/onci.23245

Flandin, L., Chang, A., Nazarenko, S., Hiltner, A., & Baer, E. (2000). Effect of strain on the properties of an ethylene-octene elastomer with conductive carbon fillers. *Journal of Applied Polymer Science*, *76*(6), 894–905. https://doi.org/10.1002/(SICI)1097-4628(20000509)76:6<894::AID-APP16>3.0.CO;2-K

Han, Z., & Fina, A. (2011). Thermal conductivity of carbon nanotubes and their polymer nanocomposites: A review. *Progress in Polymer Science (Oxford)*, *36*(7), 914–944. https://doi.org/10.1016/j.progpolymsci.2010.11.004

Hasnaoui, M. El, Kreit, L., Costa, L. C., & Achour, M. E. (2017). Investigations of Temperature Effect on the Conduction Mechanism of Electrical Conductivity of Copolymer / Carbon Black Composite, *47*(3), 121–125.

Ho, X., & Wei, J. (2013). Films of carbon nanomaterials for transparent conductors. *Materials*, *6*(6), 2155–2181. https://doi.org/10.3390/ma6062155

Hocheng, H., & Chen, C. M. (2014). Design, fabrication and failure analysis of stretchable electrical routings. *Sensors (Switzerland)*, *14*(7), 11855–11877. https://doi.org/10.3390/s140711855

Jacobson, M. Z., Delucchi, M. A., Bazouin, G., Bauer, Z. A. F., Heavey, C. C., Fisher, E., … Yeskoo, T. W. (2015). Gwent Electronic Materials Company History. *Energy Environ. Sci.*, *8*(7), 2093–2117. Retrieved from http://xlink.rsc.org/?DOI=C5EE01283J

Jandel Engineering Four Point Probing System. (2017). Retrieved May 5, 2018, from http://www.bridgetec.com/

Kiang, C., Iii, W. A. G., Beyers, R., & Bethune, D. S. (1995). Carbon Single-Layer, *33*(7), 903–914.

Li, Q., Xue, Q. Z., Gao, X. L., & Zheng, Q. B. (2009). Temperature dependence of the electrical properties of the carbon nanotube/polymer composites. *Express Polymer Letters*, *3*(12), 769–777. https://doi.org/10.3144/expresspolymlett.2009.95

Lin, C., & Chung, D. D. L. (2007). Effect of carbon black structure on the effectiveness of carbon black thermal interface pastes. *Carbon*, *45*(15), 2922–2931. https://doi.org/10.1016/j.carbon.2007.10.006

Lukes, J. R., & Zhong, H. (2007). Thermal Conductivity of Individual Single-Wall Carbon Nanotubes. *Journal of Heat Transfer*, *129*(6), 705. https://doi.org/10.1115/1.2717242

Mantena, K., Li, J., & Lumpp, J. K. (2008). Electrically Conductive Carbon Nanotube Adhesives on Lead Free Printed Circuit Board Surface Finishes. *2008 IEEE Aerospace Conference*, 1–5. https://doi.org/10.1109/AERO.2008.4526480

Merilampi, S., Laine-Ma, T., & Ruuskanen, P. (2009). The characterization of electrically conductive silver ink patterns on flexible substrates. *Microelectronics Reliability*, *49*(7), 782–790. https://doi.org/10.1016/j.microrel.2009.04.004

Nanda, M. (2008). Physico-mechanical and electrical properties of conductive carbon black reinforced chlorosulfonated polyethylene vulcanizates. *eXPRESS Polymer Letters*, *2*(12), 855–865. https://doi.org/10.3144/expresspolymlett.2008.100

Notes, A. (2015). ELECTRIC, 1–3.

Odom, S. A., Chayanupatkul, S., Blaiszik, B. J., Zhao, O., Jackson, A. C., Braun, P. V., … Moore, J. S. (2012). A self-healing conductive ink. *Advanced Materials*, *24*(19), 2578–2581. https://doi.org/10.1002/adma.201200196

Oskouyi, A. B., Sundararaj, U., & Mertiny, P. (2014). Effect of Temperature on Electrical

Resistivity of Carbon Nanotubes and Graphene Nanoplatelets Nanocomposites. *Journal of Nanotechnology in Engineering and Medicine*, *5*(4), 44501. https://doi.org/10.1115/1.4030018

Pramanik, P. K., Khastagir, D., & Saha, T. N. (1993). Effect of extensional strain on the resistivity of electrically conductive nitrile-rubber composites filled with carbon filler. *Journal of Materials Science*, *28*(13), 3539–3546. https://doi.org/10.1007/BF01159835

Pu, N.-W., Peng, Y.-Y., Wang, P.-C., Chen, C.-Y., Shi, J.-N., Liu, Y.-M., … Chang, C.-L. (2014). Application of nitrogen-doped graphene nanosheets in electrically conductive adhesives. *Carbon*, *67*, 449–456. https://doi.org/10.1016/j.carbon.2013.10.017

Qi, H. J., & Boyce, M. C. (2004). Stress-Strain Behavior of Thermoplastic Polyurethane. *Mechanics of Materials*, (July), 1–51.

Rolf Klein. (2011). Material Properties of Plastics. *Laser Welding of Plastics: Materials, Processes and Industrial Applications*, 3–69. https://doi.org/10.1002/9783527636969

Sau, K. P., Chaki, T. K., & Khastgir, D. (1998). The change in conductivity of a rubber-carbon black composite subjected to different modes of pre-strain. *Composites Part A: Applied Science and Manufacturing*, *29*(4), 363–370. https://doi.org/10.1016/S1359-835X(97)00100-0

Sau, K. P., Khastgir, D., & Chaki, T. K. (1998). Electrical conductivity of carbon black and carbon fibre filled silicone rubber composites. *Die Angewandte Makromolekulare Chemie*,*258*(4496), 11–17.https://doi.org/10.1002/(SICI)1522-9505(19980801)258:1<11::AID-APMC11>3.0.CO;2-0

Sharma, S. (2016). Development and characterization of segmented polyurethanes based on L-amino acid based chain extenders Swati Sharma, (February).

Stephens, H. L. (n.d.). *Elastomers*.

Suikkola, J. (2015). Printed Stretchable Interconnects for Wearable Health and Wellbeing

Applications, (June), 59.

Svanholm, E. (2007).*Printability and ink-coating interactions in inkjet printing*. Retrievedfromhttp://kau.diveporatl.org/smash/record.jsf?pid=diva2;6256%5Cnww

Technology, M. (2013). Influence of low – structure carbon black on the electrical , rheological and mechanical properties of graphite nanoplatelets / ethyl butyl acrylate composites Supervisor :

Thostenson, E. (2001). Advances in the science and technology of carbon nanotubes and their composites: a review. *Composites Science and Technology*, *61*(13), 1899–1912

Trinidad, J. (2016). Evaluation of Hybrid Electrically Conductive Adhesives.

Vaccarini, L., Goze, C., Henrard, L., Hernández, E., Bernier, P., & Rubio, A. (2000). Mechanical and electronic properties of carbon and boron-nitride nanotubes. *Carbon*, *38*(11), 1681–1690. https://doi.org/10.1016/S0008-6223(99)00293-

APPENDIX A

ASTM F390 Standard Test Method for Sheet Resistance

Designation: F390 – 11

Standard Test Method for Sheet Resistance of Thin Metallic Films With a Collinear Four-Probe Array[1]

This standard is issued under the fixed designation F390; the number immediately following the designation indicates the year of original adoption or, in the case of revision, the year of last revision. A number in parentheses indicates the year of last reapproval. A superscript epsilon (ε) indicates an editorial change since the last revision or reapproval.

1. Scope

1.1 This test method covers the measurement of the sheet resistance of metallic thin films with a collinear four-probe array. It is intended for use with rectangular metallic films between 0.01 and 100 μm thick, formed by deposition of a material or by a thinning process and supported by an insulating substrate, in the sheet resistance range from 10^{-2} to 10^{4} Ω/□ (see 3.1.3).

1.2 This test method is suitable for referee measurement purposes as well as for routine acceptance measurements.

1.3 The values stated in SI units are to be regarded as the standard. The values given in parentheses are for information only.

1.4 *This standard does not purport to address the safety concerns, if any, associated with its use. It is the responsibility of whoever uses this standard to consult and establish appropriate safety and health practices and determine the applicability of regulatory limitations prior to use.*

2. Referenced Documents

2.1 *ASTM Standards:*[2]

E2251 Specification for Liquid-in-Glass ASTM Thermometers with Low-Hazard Precision Liquids

F388 Method for Measurement of Oxide Thickness on Silicon Wafers and Metallization Thickness by Multiple-Beam Interference (Tolansky Method) (Withdrawn 1993)[3]

3. Terminology

3.1 *Definitions:*

3.1.1 *thin film*—a film having a thickness much smaller than any lateral dimension, formed by deposition of a material or by a thinning process.

3.1.2 *thin metallic film*—a thin film composed of a material or materials with resistivity in the range from 10^{-8} to 10^{-3} Ω·cm.

3.1.3 *sheet resistance, R_s[Ω/□]— in a thin film*, the ratio of the potential gradient parallel to the current to the product of the current density and the film thickness; in a rectangular thin film, the quotient of the resistance, measured along the length of the film, divided by the length, *l*, to width, *w*, ratio. The ratio *l*/*w* is the number of squares.

4. Summary of Test Method

4.1 A collinear four-probe array is used to determine the sheet resistance by passing a measured direct current through the specimen between the outer probes and measuring the resulting potential difference between the inner probes. The sheet resistance is calculated from the measured current and potential values using correction factors associated with the geometry of the specimen and the probe spacing.

4.2 This test method includes procedures for checking both the probe assembly and the electrical measuring apparatus.

4.2.1 The spacings between the four probe tips are determined from measurements of indentations made by the tips in a suitable surface. This test also is used to determine the condition of the tips.

4.2.2 The accuracy of the electrical measuring equipment is tested by means of an analog circuit containing a known standard resistor together with other resistors which simulate the resistance at the contacts between the probe tips and the film surface.

5. Apparatus

5.1 *Probe Assembly:*

5.1.1 *Probes*—The probe shaft and tip shall be constructed of tungsten carbide, Monel, hardened tool steel, or hard copper and have a conical tip with included angle of 45 to 90°. Alternatively, the tip may be formed from a platinum-palladium alloy and resistance welded to the shaft. The tip shall have a nominal initial radius of 25 to 50 μm. In all cases all of

[1] This test method is under the jurisdiction of ASTM Committee F01 on Electronics and is the direct responsibility of Subcommittee F01.17 on Sputter Metallization.

Current edition approved June 1, 2011. Published July 2011. Originally approved in 1973 as F390 – 73 T. Last previous edition approved in 2003 as F390 – 98(2003). DOI: 10.1520/F0390-11.

[2] For referenced ASTM standards, visit the ASTM website, www.astm.org, or contact ASTM Customer Service at service@astm.org. For *Annual Book of ASTM Standards* volume information, refer to the standard's Document Summary page on the ASTM website.

[3] Withdrawn. THe last approved version of this historical standard is referenced on www.astm.org.

APPENDIX A

ASTM F390 Standard Test Method for Sheet Resistance

the four paths from the electrical measurement equipment inputs to the film surface must be identical.

5.1.2 *Probe Force*—The probes shall be uniformly loaded to exert a force sufficient to deform the metal film but insufficient to puncture the film. A rough guide for loading is a load of 20 g/Mohs (unit of hardness) of the film material on each probe.

5.1.3 *Probe Characteristics*—The probes shall be mounted in an insulating fixture such as a sapphire bearing in a methyl methacrylate or hardened polystyrene block in an equally spaced linear array. The electrical insulation between adjacent probe points shall be at least 10^5 times greater than the *V/I* ratio of the film. The spacing shall be 0.64 to 1.00 mm inclusive (0.025 to 0.040 in. inclusive) as agreed upon between the parties concerned with the test. The precision and reproducibility of the probe spacing shall be established according to the procedure of 7.1.

5.1.4 *Probe Support*—The probe support shall allow the probes to be lowered perpendicularly onto the surface of the specimen so that the center of the array is centered on the specimen within ±10 % of the specimen length *l* and width *w*.

5.2 *Electrical Measuring Apparatus:*

5.2.1 The electrical apparatus shall consist of a suitable voltmeter, current source, ammeter, and electrical connections (see 7.2).

5.2.2 *Voltmeter* with input impedance 10^4 times the *V/I* ratio of the film. A vacuum-tube voltmeter, a digital voltmeter, or similar high-impedance input apparatus is suitable.

5.2.3 *Current Source* with current regulation and stability of ±0.1 % or better. The recommended current range is from 0.01 to 100 mA.

5.2.4 *Ammeter* capable of reading direct current in the range from 0.01 to 100 mA to an accuracy of ±0.1 % or better.

5.2.5 The current source and ammeter are connected to the outer probes; the voltmeter is connected to the inner probes.

5.3 *Specimen Support*—A copper block at least 100 mm (approximately 4 in.) in lateral dimensions and at least 40 mm (approximately 1.5 in.) thick, shall be used to support the specimen and provide a heat sink. It shall contain a hole that will accommodate a thermometer (see 5.4) in such a manner that the center of the bulb of the thermometer shall be not more than 10 mm below the central area of the top of the block where the specimen is to be placed.

5.4 *Thermometer* having a range from – 8 to 32°C and conforming to the requirements for Thermometer 63C as prescribed in Specification E2251.

5.5 *Vernier Calipers.*

5.6 *Toolmaker's Microscope* capable of measuring increments of 2.5 µm.

6. Test Specimen

6.1 The specimen shall consist of a continuous rectangular thin metallic film with a thickness greater than 0.01 µm and less than 100 µm. Thickness variation shall be less than ±10 % of the nominal thickness for thickness from 0.01 µm to 0.1 µm, inclusive; for greater thicknesses, the variation shall be less than ±5 % of the nominal thickness. The specimen shall be used as prepared by deposition of a material or by a thinning process, with no further cleaning or preparation. The test specimen shall be supported by a substrate consisting of a suitable insulating material.

6.2 *Geometry*—Measure the length, *l*, and width, *w*, of the specimen with vernier calipers. Record the values.

6.3 Measure the thickness, *t*, of the film in accordance with Method F388.

7. Suitability of Test Equipment

7.1 *Probe Assembly*—The probe spacing and tip condition shall be established in the following manner. It is recommended that this be done immediately prior to a referee measurement.

7.1.1 *Procedure:*

7.1.1.1 Make a series of indentations on the surface of the specimen to be tested or other surface of similar hardness with the four-probe array. Make these indentations by applying the probes to the surface using normal point pressures. Lift the probes and move either the specimen surface or the probes 0.05 to 0.10 mm in a direction perpendicular to a line through the probe tips. Again apply the probes to the specimen surface. Repeat the procedure until a series of ten indentation sets is obtained.

NOTE 1—It is recommended that the surface or the probes be moved twice the usual distance after every second or every third indentation set in order to assist the operator in identifying the indentations belonging to each set.

7.1.1.2 Place the specimen so indented on the stage of the toolmaker's microscope so that the *Y*-axis readings (Y_A and Y_B in Fig. 1) do not differ by more than 0.15 mm (0.006 in.). For each of the ten indentation sets record the readings *A* through *H* (defined in Fig. 1) on the *X*-axis of the toolmaker's microscope and the readings Y_A and Y_B on the *Y*-axis.

7.1.2 *Calculations:*

7.1.2.1 For each of the ten sets of measurements calculate the probe separations, S_{1j}, S_{2j}, and S_{3j} from the equations:

$$S_{1j} = [(C_j + D_j)/2] - [(A_j + B_j)/2],$$

$$S_{2j} = [(E_j + F_j)/2] - [(C_j + D_j)/2], \text{ and}$$

$$S_{3j} = [(G_j + H_j)/2] - [(E_j + F_j)/2]$$

where the index *j* is the set number and has a value from 1 to 10.

7.1.2.2 Calculate the average value for each of the three separations using the S_{ij} calculated above and the equation:

$$\bar{S}_i = \left(\frac{1}{10}\right)\sum_{j=1}^{10} = S_{ij}$$

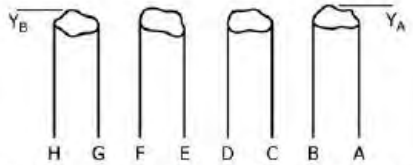

FIG. 1 Measurement Locations for Typical Probe Indentation Pattern

APPENDIX A

ASTM F390 Standard Test Method for Sheet Resistance

where the index i successively takes the values 1, 2, and 3 (see 7.1.2.1).

7.1.2.3 Calculate the sample standard deviation s_i for each of the three separations using the $\bar{S}_i$ calculated in 7.1.2.2, the S_{ij} calculated in 7.1.2.1, and the equation:

$$s_i = \left(\frac{1}{3}\right)\left[\sum_{j=1}^{10}\left(S_{ij} - \bar{S}_i\right)^2\right]^{1/2}$$

7.1.2.4 Calculate the average probe spacing $\bar{S}$ as follows:

$$\bar{S} = \left(\frac{1}{3}\right)\left(\bar{S}_1 + \bar{S}_2 + \bar{S}_3\right)$$

7.1.2.5 Calculate the probe spacing correction factor F_{sp} as follows:

$$F_{sp} = 1 + 1.082\left[1 - \left(\bar{S}_2/\bar{S}\right)\right]$$

7.1.3 *Requirements*—For the probe assembly to be acceptable it must meet the following requirements:

7.1.3.1 Each of the three sets of ten measurements for S_i shall have a sample standard deviation s_i of less than 1 % of $\bar{S}_i$.

7.1.3.2 The average values of the separations ($\bar{S}_1$, $\bar{S}_2$, and $\bar{S}_3$) shall not differ by more than 5 % of $\bar{S}$.

7.1.3.3 The probe indentations shall not puncture the film.

7.2 *Electrical Equipment*—The suitability and accuracy of the electrical equipment shall be established in the following manner. It is recommended that this be done immediately prior to a referee measurement.

7.2.1 Measure the current through and voltage across a standard resistor whose resistance value is within a factor of ten of the *V/I* ratio of the film to be measured. Perform ten times.

7.2.2 Calculate the resistance r_i for the ratio of voltage to current for each measurement.

7.2.2.1 Calculate the average resistance $\bar{r}$ as follows:

$$\bar{r} = \left(\frac{1}{10}\right)\sum_{j=1}^{10} r_i$$

where:

r_i = one of the ten values of resistance determined in 7.2.1.

7.2.2.2 Calculate the sample standard deviation as follows:

$$s_r = \left(\frac{1}{3}\right)\left[\sum_{j=1}^{10}\left(r_i - \bar{r}\right)^2\right]^{1/2}$$

7.2.3 *Requirements*—For the electrical measuring equipment to be suitable, it must meet the following requirements:

7.2.3.1 The value of $\bar{r}$ must be within 1.0 % of the known value of r.

7.2.3.2 The sample standard deviation s_r must be less than 1.0 % of $\bar{r}$.

7.2.3.3 The resolution of the equipment must be such that differences in resistance of 0.05 % can be detected.

8. Procedure

8.1 Connect the voltage measuring apparatus to the two center probes.

8.2 Connect the current source to the outer two probes.

8.3 Equilibrate the specimen at room temperature (23± 2°C) on the heat-sink block. Record the temperature.

8.4 Place the test specimen on the mounting block under the probe with the length parallel to the line of the probe array to within± 2°. Lower the probe onto the test specimen ensuring that the center of the probe array is centered on the specimen within ±10 % of the specimen length l and width w. Establish a current (see 8.5.1) between the outer probes. Record the voltage and current. Perform ten times.

8.5 *Caution*—Spurious and inaccurate results can arise from a number of sources.

8.5.1 It is recommended that, consistent with the desired accuracy, the applied current be as low as possible to reduce specimen heating. In high resistance or very thin films, it may be desirable to reduce the specimen current to prevent resistance heating. A drifting of the voltage reading may indicate a change in the resistance due to heating.

8.5.2 Wear and deformation of the tips in use may make frequent inspection and replacement necessary.

8.5.3 Spurious currents can be introduced into the test specimen by high-frequency generators. If equipment is used near such sources, adequate shielding should be provided.

9. Calculations

9.1 Calculate the specimen resistance R_i from the ratio of measured voltage and current.

9.2 Calculate the average specimen resistance $\bar{R}$ as follows:

$$\bar{R} = \left(\frac{1}{10}\right)\sum_{j=1}^{10}\bar{R}_i$$

9.3 Calculate the sample standard deviation as follows:

$$s = \left(\frac{1}{3}\right)\left[\sum_{j=1}^{10}\left(R_i - \bar{R}\right)^2\right]^{1/2}$$

9.3.1 *Requirement*—For acceptance of the resistance, the sample standard deviation s shall be less than 1 % of $\bar{R}$.

9.4 Calculate the ratio of the specimen width w (see 6.2) to the average probe separation $\bar{S}$ (see 7.1.2.4). Calculate the ratio of specimen length l to specimen width w. Determine the lateral correction factor c from Table 1 by means of linear interpolation.

TABLE 1 Lateral Correction Factor, c, for Rectangular Thin Films

w/S	ℓ /w = 1	ℓ /w = 2	ℓ /w = 3	ℓ /w = 4
1.00	...	...	0.9988	0.9994
1.25	...	...	1.2467	1.2248
1.50	...	1.4788	1.4893	1.4893
1.75	...	1.7196	1.7238	1.7238
2.00	...	1.9454	1.9475	1.9475
2.50	...	2.3532	2.3541	2.3541
3.00	2.4575	2.7000	2.7005	2.7005
4.00	3.1137	3.2246	3.2248	3.2248
5.00	3.5098	3.5749	3.5750	3.5750
7.50	4.0095	4.0361	4.0362	4.0362
10.00	4.2209	4.2357	4.2357	4.2357
15.00	4.3882	4.3947	4.3947	4.3947
20.00	4.4516	4.4553	4.4553	4.4553
40.00	4.5190	4.5129	4.5129	4.5129
∞	4.5324	4.5324	4.5324	4.5324

APPENDIX A

ASTM F390 Standard Test Method for Sheet Resistance

9.5 Calculation the ratio of the film thickness t (see 6.3) to the average probe separation $\bar{S}$ (see 7.1.2.4). Find the correlation factor $F(t/\bar{S})$ from Table 2 by means of linear interpolation.

9.6 Calculate the geometrical correction factor F as follows:

$$F = c \times F\left(t/\bar{S}\right) \times F_{sp}$$

where

F_{sp} = probe spacing correction factor (see 7.1.2.5).

9.7 Calculate the sheet resistance R_s as follows:

$$R_s = \bar{R} \times F$$

10. Report

10.1 For a referee test the report shall include the following:

10.1.1 A description of the specimen, including:

10.1.1.1 Type of film,

10.1.1.2 Specimen identification,

10.1.1.3 Color,

10.1.1.4 Appearance,

10.1.1.5 Source, and

10.1.1.6 Previous treatment and tests.

10.1.2 Dimensions and data, including:

10.1.2.1 Length and width,

10.1.2.2 Average values and standard deviations of probe spacing,

10.1.2.3 Standard resistor value,

10.1.2.4 Measured average value and standard deviation of standard resistor, and

10.1.2.5 Temperature.

10.1.3 Measured values of current and voltage.

10.1.4 Calculated average value and standard deviation of resistance.

10.1.5 Values of correction factors used.

10.1.6 Calculated value of room temperature sheet resistance.

10.2 Fur a routine test only such items as are deemed significant by the parties to the test need be reported.

TABLE 2 Thickness Correction Factor for Thin Films

t/S	F(t/S)
0.4000	0.9995
0.5000	0.9974
0.5555	0.9948
0.6250	0.9898
0.7143	0.9798
0.8333	0.9600
1.0000	0.9214
1.1111	0.8907
1.2500	0.8490
1.4286	0.7938
1.6666	0.7225
2.0000	0.6336

11. Precision and Bias

11.1 *Precision*—A two-laboratory comparative test of the measurement of sheet resistance on two groups of thin metallic films using separate pieces of equipment has yielded agreement to within ±0.44 % of the average value for sheet resistance values in the range from 25 to 40 Ω/ ^{2} and ±1.7 % for sheet resistance values in the range from 0.010 to 0.060 Ω/^{2}.

11.1.1 *Precision*—Subcommittee F01.17 will conduct an interlaboratory test to confirm the precision of this test method.

11.2 *Bias*—Since there is no accepted reference material suitable for determining the bias for the procedure in this test method, bias has not been determined.

12. Keywords

12.1 collinear four-point probe; electrical resistance; electrical sheet resistance; four-point probe; resistance; thin films; thin conductive films; thin metallic films

APPENDIX C1

Data Sheet for Carbon Black Bare Conductive Ink

BARE CONDUCTIVE®

ELECTRIC PAINT®

Application Notes

PRODUCT DESCRIPTION

Electric Paint is available in 10ml pens and 50ml jars. It is a nontoxic, water based, water soluble, electrically conductive paint. **Electric Paint** adheres to a wide variety of substrates and is easily removed with water. It is black in color and can be over- painted with any material compatible with a water-based paint. Please see the **Electric Paint** MSDS for precautionary information.

ADVANTAGES / PRODUCT BENEFITS

- Electrically conductive
- Nontoxic
- Water-soluble
- Works with low voltage DC power sources at low currents (see "Power Sources" p.2) Powers small devices
- Can be used as a potentiometer
- Compatible with many standard printing processes

TYPICAL PROPERTIES

Color /	Black
Viscosity /	Highly viscous and shear sensitive (thixotropic)
Density /	1.16 g/ml
Surface Resistivity /	55 Ω/Sq @ 50 microns or 32 Ω/Sq when using a brush (see p.3)
Vehicle /	Water-based
Use by /	6 months after opening
Drying Temperature /	**Electric Paint** should be allowed to dry at room temperature for 5 – 15 minutes. Drying time can be reduced by placing **Electric Paint** under a warm lamp or other low intensity heat source.

Bare Conductive Ltd
First Floor, 98 Commercial St
London E1 6LZ
United Kingdom

tel +44 0 207 650 7977
fax +44 0 203 002 4697
info@bareconductive.com
bareconductive.com

APPENDIX C2

Data Sheet Singlewalled for Carbon Nanotubes Conductive Ink

SIGMA-ALDRICH

792462 ALDRICH

Carbon nanotube, single-walled, solvent-based conductive ink, SWCNT

1 mg/mL

Synonym: SWCNT Ink, SWNT Ink, SWeNT V2V ink, SWeNT VC101 ink, Single-Walled Carbon Nanotube Ink, conductive ink

SDS

POPULAR DOCUMENTS: SPECIFICATION SHEET (PDF)

Properties

Related Categories	3D Printing Materials for Research and Development, Carbon Nanomaterials, Carbon Nanotubes, Conductive Inks for 3D Printing, Inks for Printing Applications, More...
form	viscous liquid (black)
concentration	1 mg/mL
sheet resistance	<1000 Ω/sq, by 4-point probe on prepared (at 87.5% VLT (ohm/sq))
viscosity	17.7 Pa.s(25 °C) (at 10 sec^{-1} shear rate)
storage temp.	2-8°C

Description

Packaging
25, 100 mL in glass bottle

Application
This solvent based conductive ink is primarily formulated for Screen Printing Transparent Conductors

General description
Single walled carbon nanotubes offer an alternative to metallic conductive inks. The nanotubes exhibit high conductivity, oxidation resistance. Carbon nanomaterial based conductive inks are used in printed and flexible electronics, thin film transistors, electrochemical sensors, supercapacitors and photovoltaics.

Legal Information
Product of Chasm Advanced Materials, Inc.
Signis is a registered trademark of Chasm Advanced Materials, Inc.
CoMoCAT is a trademark of Chasm Advanced Materials, Inc.
CHASM is a trademark of Chasm Advanced Materials, Inc.

Price and Availability

SKU-Pack Size	Availability	Price (USD/MYR)	Quantity
792462-25ML	Estimated to ship on 16.02.18	1,092.50	0
792462-100ML	Estimated to ship on 06.03.18	3,595.00	0

BULK ORDERS? ADD TO CART